GRAVITY RETAINING WALLS SUBJECT TO SEISMIC LOADING

GEO REPORT No. 45

Y.S. Au-Yeung & K.K.S. Ho

GEOTECHNICAL ENGINEERING OFFICE
CIVIL ENGINEERING DEPARTMENT
HONG KONG

GRAVITY RETAINING WALLS SUBJECT TO SEISMIC LOADING

GEO REPORT No. 45

Y.S. Au-Yeung & K.K.S. Ho

This report was originally produced in December 1994 as GEO Technical Note No. TN 1/94

First published, June 1995

Prepared by:

Geotechnical Engineering Office,
Civil Engineering Department,
Civil Engineering Building,
101 Princess Margaret Road,
Homantin, Kowloon,
Hong Kong.

This publication is available from:

Government Publications Centre,
Ground Floor, Low Block,
Queensway Government Offices,
66 Queensway,
Hong Kong.

Overseas orders should be placed with:

Publications (Sales) Office,
Information Services Department,
28th Floor, Siu On Centre,
188 Lockhart Road, Wan Chai,
Hong Kong.

Price in Hong Kong: HK$40
Price overseas: US$8 (including surface postage)

An additional bank charge of **HK$50** or **US$6.50** is required per cheque made in currencies other than Hong Kong dollars.

Cheques, bank drafts or money orders
must be made payable to **HONG KONG GOVERNMENT**

PREFACE

In keeping with our policy of releasing information of general technical interest, we make available some of our internal reports in a series of publications termed the GEO Report series. The reports in this series, of which this is one, are selected from a wide range of reports produced by the staff of the Office and our consultants.

Copies of GEO Reports have previously been made available free of charge in limited numbers. The demand for the reports in this series has increased greatly, necessitating new arrangements for supply. Henceforward a charge will be made to cover the cost of printing.

The Geotechnical Engineering Office also publishes guidance documents and presents the results of research work of general interest in GEO Publications. These publications and the GEO Reports may be obtained from the Government's Information Services Department. Information on how to purchase these publications is given on the last page of this report.

A. W. Malone
Principal Government Geotechnical Engineer
June 1995

FOREWORD

This Technical Note reviews the common methods of designing gravity retaining walls under earthquake excitation. In addition to assessing the dynamic earth and water pressures that may be exerted on the retaining wall, the calculation of displacement and rotation of the wall is also considered. The recommended procedure for undertaking a seismic analysis of a retaining wall is given, and a new method of assessing wall rotation has been formulated.

This Technical Note was prepared by Mr Y.S. Au Yeung, who was assisted by Mr K.K.S. Ho. The work is largely based on Mr Au Yeung's dissertation completed during his MSc course at Imperial College of Science, Technology & Medicine in the academic year 1991-92. A draft of the report was reviewed by Mr W.K. Pun and Mr S.H. Mak.

(Y.C. Chan)
Chief Geotechnical Engineer/Special Projects

CONTENTS

Page No.

1. INTRODUCTION

Retaining walls in Hong Kong are not routinely designed against earthquake loading. However, abutment walls of highway and railway bridges are generally designed for a horizontal ground acceleration of 5% g applied at the centre of gravity of the structure, with a partial load factor of 1.4 (Highways Department, 1993). This is equivalent to adopting a design horizontal acceleration of 7% g for ultimate limit state design of such structures.

Geoguide 1 (GEO, 1993) recommends that in addition to abutment walls, seismic loading should be considered specifically in the design for the following situations :

(a) retaining walls affecting high risk structures or major lifelines, e.g. power plants and trunk water mains, and

(b) cantilevered retaining walls retaining saturated materials for which positive pore water pressures can be generated and the shear strength of the soil may be adversely affected under seismic excitation (e.g. loose fill, loose colluvium, etc).

In this Technical Note, the available methods of determining dynamic earth pressure and dynamic water pressure under seismic loading on gravity retaining walls are reviewed. A range of approaches in assessing the displacement of a retaining wall are outlined, and a simplified method for estimating the wall rotation is put forward.

Based on a critical review of the literature and current overseas practice, a simplified method for designing a gravity-type retaining wall including reinforced concrete L-shaped or inverted T-shaped retaining walls, against earthquake loading is proposed for use in Hong Kong. The possible behaviour of masonry walls under seismic loading is not covered in this Technical Note.

2. EVALUATION OF DYNAMIC EARTH PRESSURE

2.1 General

The typical design condition for a gravity retaining wall subject to seismic loading is shown in Figure 1. It involves a simplified geological model for the ground in that the soil layers including saprolites are idealised as a soil column overlying less weathered rock (i.e. Grade III or better) denoted as bedrock. In general, the properties of the backfill behind the wall are different from that of the insitu soil which overlies bedrock.

The seismic vibrational energy in the bedrock propagates towards the wall through the soil layers. In order to assess the wall stability during earthquakes, it is necessary to know the earth pressure acting on the wall. The dynamic earth pressure that will be induced is influenced by a range of factors including :

(a) nature of the seismic incident wave,

(b) thicknesses of the soil layers and the wall dimensions,

(c) properties of the soil (e.g. shear wave velocity, stress-strain characteristics and density),

(d) properties of the wall material,

(e) properties of the interface boundaries (i.e. wall/soil interface and soil/rock interface),

(f) refraction and reflection characteristics of seismic waves at the boundaries of different materials, and

(g) groundwater conditions and their dynamic response under earthquake vibration.

Rigorous analyses considering all the above factors are fraught with difficulties in practice. In any case, the applicability of sophisticated analyses is limited by the uncertainties associated with material behaviour and parameter determination under dynamic conditions. Therefore, a range of analysis methodologies have been suggested in the literature based on simplifying assumptions.

The different methods can be grouped into two broad categories, namely pseudo-static approach and dynamic response analysis. These are discussed in the following.

2.2 Pseudo-static Analysis

2.2.1 General

In the conventional pseudo-static approach, the dynamic response of the wall/soil system in terms of amplification is assumed to be insignificant. The wall and the associated soil wedge are taken to behave as a rigid block. The seismic loading is considered as equivalent inertial forces, and the dynamic earth pressure is determined on the basis of static equilibrium consideration.

It should be noted that the forces that arise due to the inertia of the wall must be considered in a seismic analysis. In practice, the horizontal force is usually taken to be that given by the same design free-field acceleration coefficient taken for the ground.

2.2.2 Mononobe-Okabe Method

The earliest method for determining the combined static and dynamic earth pressure on a retaining wall was developed by Okabe (1926) and Mononobe & Matsuo (1929). This method, generally referred to as the Mononobe-Okabe method, is based on plasticity theory and is essentially an extension of the Coulomb sliding wedge theory in which the transient earthquake forces are represented by an equivalent static force. The latter is expressed in terms of the weight of the wedge multiplied by a seismic coefficient.

The method was originally developed for a dry cohesionless material with the following assumptions :

(a) the wall yields sufficiently such that a triangular soil wedge behind the wall is formed at the point of incipient failure, with the maximum shear strength mobilized along the sliding surface,

(b) the wall and the soil behave as a rigid body with the shear wave travelling at an infinite speed such that the acceleration effectively becomes uniform throughout the mass of the soil wedge.

With the above assumptions, the effect of the earthquake motion can be represented as inertial forces $K_h.W$ and $K_v.W$ acting at the centre of gravity of the mass, where W is the weight of the sliding wedge, and K_h and K_v is the horizontal and vertical ground acceleration coefficient respectively.

The principle of this method is shown in Figure 2. The expression of the total dynamic force, P_{AE}, is given below :

$$P_{AE} = \frac{1}{2}\gamma H^2 (1 + K_v)\, C_{AE} \quad \ldots\ldots\ldots\ldots\ldots\ldots \quad (1)$$

and

$$C_{AE} = \frac{\cos^2(\phi' - \theta - \beta)}{\cos\theta \, \cos^2\beta \, \cos(\delta + \beta + \theta) \left[1 + \sqrt{\dfrac{\sin(\phi' + \delta)\, \sin(\phi' - \theta - i)}{\cos(\delta + \beta + \theta)\, \cos(i - \beta)}} \right]^2} \quad \ldots\ldots \quad (2)$$

where C_{AE} = horizontal seismic coefficient
H = height of wall
K_h = horizontal ground acceleration coefficient
K_v = vertical ground acceleration coefficient
ϕ' = angle of shearing resistance of soil
δ = angle of wall friction
i = inclination of ground surface behind wall to horizontal
β = inclination of back of wall to vertical
γ = unit weight of soil
g = acceleration due to gravity
θ = inclination of the resultant inertial force to the vertical
$= \tan^{-1} \left(\dfrac{K_h}{1 + K_v}\right)$

For walls with a vertical back retaining level backfill, the variation of C_{AE} with K_h (assuming K_v=0) is shown in Figures 3 to 5 for ϕ' varying from 32° to 40°, and a δ of 0, $\phi'/2$ and $2/3\phi'$ respectively. These cover the range of typical parameters for Hong Kong soils under static conditions. Any possible increase in shear strength due to the strain rate effects under dynamic loading condition, or possible reduction in shear strength due to cyclic nature of earthquake loading has been ignored.

The pseudo-static approach can be visualized as effectively tilting the ground profile and wall geometry by an angle θ (defined as above), with a new gravity, g', given by the following equation :

$$g' = \sqrt{(1+K_v)^2 + K_h^2}\, g \qquad \ldots\ldots\ldots\ldots\ldots\ldots (3)$$

It must be emphasized that the Mononobe-Okabe formula is limited in its application to dry cohesionless soils with a simple geometry. A number of parameters such as soil cohesion, wall adhesion, irregular ground profile, surcharge and water pressure which may be relevant for many wall structures in Hong Kong, cannot be directly allowed for.

It should be noted that the Mononobe-Okabe equation is applicable for retaining walls where the angle i is less than or equal to (ϕ' - θ). This is because if the angle i is greater than (ϕ' - θ), the sloping backfill behind the wall will be unstable unless the soil has sufficient cohesive strength. In the latter case, the more versatile trial wedge analysis approach as discussed in the following section should be adopted.

2.2.3 Trial Wedge Analysis

The trial wedge analysis is based on the same principal assumptions of the Mononobe-Okabe method. This approach is essentially an extension of the conventional trial wedge method for static earth pressure problems, the only difference being the inclusion of additional horizontal and vertical forces (i.e. K_h.W and K_v.W respectively). The basic principle of this method is illustrated in Figure 6.

As shown in the complex force polygon in Figure 6, the trial wedge method is much more tedious than the Mononobe-Okabe method. In order to facilitate computation, a computer program has been developed using Microsoft Quick Basic language.

An example of a problem which cannot be solved by the Mononobe-Okabe formula but which can easily be handled by the trial wedge program is shown in Figure 7. The problem involves an irregular ground surface subjected to a strip surcharge and a point load. The soil has a cohesion component. Also, any dynamic pore water pressures generated during earthquake shaking can be allowed for. The estimation of dynamic pore water pressure is discussed in Section 3.

2.2.4 Wall with Saturated Clay Backfill

For walls retaining clay backfill, the following guideline is given by Pappin (1992) for calculating the total dynamic force :

$$P_{AE} = \frac{0.5\gamma\ H^2 \sin(\eta+\theta)}{\cos\theta\ \sin\eta} - \frac{c_u}{\cos\eta\ \sin\eta} \quad \text{.............} \quad (4)$$

where c_u = undrained shear strength

$$\eta = \tan^{-1}\sqrt{1-\frac{(\gamma H)\ \tan\theta}{2c_u}}$$

$$\theta = \tan^{-1}\left(\frac{K_h}{1+K_v}\right)$$

and the other terms are defined in Section 2.2.2.

In general, it is very difficult to estimate the appropriate undrained shear strength under dynamic conditions as this parameter depends on a number of factors including strain rate, stress history, characteristics of the vibration, etc. An alternative approach would be to adopt the trial wedge method if the dynamic pore water pressure can be estimated with reasonable certainty.

More work needs to be done on assessing the best means to determine the dynamic c_u and the dynamic earth pressure arising from a clay backfill.

2.2.5 Vertical Ground Acceleration

The vertical component of ground acceleration is normally a fraction of the horizontal component of ground acceleration. In principle, although vertical acceleration may increase the active pressure on the wall, it also increases the sliding and overturning resistance (but not bearing).

In the epicentral area, the vertical peak ground acceleration can be quite high, but as the distance from the epicentre increases, it tends to reduce. The vertical component of ground acceleration is usually neglected in pseudo-static seismic stability analysis based on the following considerations :

(a) The chance of a site being located near the earthquake epicentre is low, and hence the vertical peak ground acceleration is expected to be small compared with the horizontal peak ground acceleration.

(b) The vertical and horizontal peak ground accelerations normally do not occur at the same time.

(c) The vertical ground motion is usually of a higher frequency, and hence there are balancing effects between the upward and downward vertical inertia forces resulting from such motions.

For general design purposes, it is customary to ignore the effects due to vertical ground acceleration, as adopted in the Codes of Practice by countries such as Japan and New Zealand.

2.2.6 Point of Application of Dynamic Force from the Ground

If the ground behind the wall is uniform, the pseudo-static analysis will give the point of application of the dynamic force at $^1/_3$ height above the bottom of the wall. However, this is questionable because the pseudo-static method strictly only considers force equilibrium and not moment equilibrium. Results of previous model tests as summarised by Prakash & Nandkuamaran (1973) showed that the point of application generally lies between $^1/_3$ H and $^2/_3$ H, where H is the height above the bottom of the wall.

In view of the uncertainties concerning the point of application, it is suggested that the dynamic force from the ground can be conservatively assumed to lie at $^2/_3$ above the bottom of the wall for practical purposes.

2.2.7 Dynamic Pressure on Rigid Wall

Caution should be exercised in applying the Mononobe-Okabe's solution or the trial wedge method for unyielding walls. In this case, the dynamic thrust can be substantially under-estimated by these simplified methods because there may be insufficient deformation of the backfill for full mobilisation of shear resistance along the failure plane on the active side. Dorwick (1987) recommends that for walls restrained against outward movement, the design earth pressure should be taken as the sum of the static pressure behind the wall and $K_h \gamma H^2$.

2.2.8 Dynamic Passive Earth Pressure

Assuming a sliding block bounded by a planar failure surface, the dynamic passive thrust on the wall, P_{PE}, is given by the following (Nadim & Whitman, 1993) :

$$P_{PE} = \frac{1}{2} K_{PE} \, \gamma \, (1 - K_v) \, H^2 \quad \ldots\ldots\ldots\ldots\ldots\ldots \quad (5)$$

and

$$K_{PE} = \frac{\cos^2(\phi' - \theta + \beta)}{\cos\theta \, \cos^2\beta \, \cos(\delta - \beta + \theta) \left[1 - \sqrt{\dfrac{\sin(\phi' + \delta)\,\sin(\phi' - \theta + \iota)}{\cos(\iota - \beta)\,\cos(\theta - \beta + \delta)}} \right]^2}$$

where the symbols are defined in Section 2.2.2.

It should be noted that maximum P_{PE} occurs when the ground acceleration is acting away from the backfill. The above formulation suffers from the shortcoming that a more critical mode of failure may correspond to that given by a curved surface of sliding. Thus, the above will potentially give an unsafe solution. More work needs to be done in the evaluation of a rational method to determine the value of P_{PE} if passive resistance is important for the stability of the structure.

Due to the above shortcoming and in order to err on the conservative side, the contribution from the dynamic passive force is frequently ignored.

2.3 Dynamic Response Analysis

In a dynamic response analysis, the dynamic behaviour of the soil-structure system, dynamic material properties, and the nature of seismic waves are characterised by different models. Using this more sophisticated method of analysis, a number of factors can be investigated including the effects of deformability of the founding soil and the backfill, frequency of seismic excitation, possible amplification, etc.

Different formulations have been suggested in the literature. Byrne & Salgado (1981) modelled the soil using elasto-plastic springs and the equation of motion is solved in a step-by-step manner in the time domain. Steedman & Zeng (1990) proposed a simplified method for assessing the earth pressure, taking into account the nature of the seismic wave and their mode of propagation. The use of numerical techniques, such as the finite-element method, to tackle dynamic problems has been described by Aggour & Brown (1979).

2.4 Residual Increase in Static Pressure After Seismic Excitation

Using the finite element method, Nadim & Whitman (1984) computed a residual thrust remaining at the end of seismic excitation over and above the static force. Similar observations were made in a UDEC (Universal Distinct Element Code) analysis of a caisson wall by Wong & Li (1994). Other researchers have also reported such observations in laboratory tests, e.g. Steedman (1984), Yong (1985), Anderson et al (1987), and Stamatopoulos & Whitman (1990).

Nadim & Whitman (1993) postulated that such a residual increase in pressure may be associated with the tendency for sand to densify when it is subject to shaking, with attendant increase in the minor principal stress.

In current practice, the residual pressure after seismic excitation is seldom considered in a conventional analysis. It seems that so long as no collapse or significant damage is sustained by the structure under a severe earthquake, the increase in structural forces in the wall structure which may lead to cracking can be tolerated in design.

2.5 Discussion on Approaches of Analyses

The dynamic response approach is theoretically more accurate than the pseudo-static approach as the former can, in principle, better model the dynamic features of the system. However, the results of dynamic response analyses are very sensitive to the input parameters, which are generally difficult to determine with certainty. Such parameters include the nature of the strong-motion, the stress-strain relationship of the soil under cyclic loading, damping characteristics at the boundaries, etc. It should be noted that there are no known Codes of Practice which explicitly stipulate typical situations where dynamic response analyses are warranted.

Given the difficulties associated with the more sophisticated analyses and the uncertainties concerning their validity, dynamic response analyses are usually not justified for analysis of conventional gravity retaining walls subjected to earthquake loading. Their use is still restricted to research purposes or exceptional projects where they can provide an insight into the relative importance of the different parameters.

On the other hand, there is much experimental evidence suggesting that lateral pressure coefficients for cohesionless backfill computed by the pseudo-static approach compare favourably with the test results observed in model tests in dry sand subjected to a ground acceleration of up to about 40% g (Prakash & Nandkuamaran, 1973).

For seismic design of gravity retaining walls, the pseudo-static analysis with appropriate choice of the design seismic coefficient and factors of safety is considered adequate. This approach has been adopted by a number of countries with a high level of seismicity such as Japan, which has much experience in the design of earthquake-resistant structures. Overall, it seems reasonable to adopt the trial wedge approach or Mononobe-Okabe method for gravity-type retaining walls where movements is likely to be sufficient to achieve the active state.

3. EVALUATION OF WATER PRESSURE UNDER DYNAMIC CONDITIONS

3.1 General

The prediction of dynamic pore water pressure in saturated soils is very complicated. The principal difficulty lies in formulating a simple, but realistic, model which takes into account all relevant factors, such as dynamic viscosity, permeability, interaction between soil particles and water, and deformation of the soil skeleton. Only limited work has previously been done to address this problem in a rigorous manner.

The mechanism associated with the change in pore water pressure caused by earthquake shaking is illustrated in Figure 8. When the soil sample is subjected to a ground acceleration $K_h.g$, the soil particles can be assumed to take up the same acceleration if the mass is small or where the seismic wave travels very fast relative to the scale of the mass.

When the interstices between soil particles are very small, the water will be effectively entrapped and no flow of water is anticipated. However, if the pore sizes are large, the water will not attain the soil particle acceleration instantaneously due to its limited rigidity. Therefore, the water will tend to leave the interstices and shear stresses will be generated as a result of dynamic viscosity of water. The soil skeleton may deform due to changes in shear stress, which in turn may give rise to changes in the pore water pressure. Thus, a rigorous analysis must allow for the possible coupled water flow and shear deformation of the soil under earthquake shaking.

As the permeability of the material decreases, it becomes more difficult to evaluate the effective stresses and pore pressures separately. With very small permeability, undrained conditions will prevail. Moreover, it should be noted that excess pore pressures may be generated cumulatively as a result of cyclic straining.

In practice, it is suggested that the following two principal mechanisms of generation of dynamic water pressures should be assessed separately :

(a) hydrodynamic pressure due to movement of water, and

(b) dynamic pore water pressure due to deformation of the soil skeleton upon shearing.

3.2 Hydrodynamic Pressure

3.2.1 Free Standing Water

Examples of this type of problem include dynamic water pressure on reservoir dams and on seawalls. Using the theory of hydrodynamics for hydraulic wave propagation, Westergaard (1933) conducted a rigorous analysis of the pressure distribution on a dam structure undergoing horizontal sinusoidal oscillations.

According to Westergaard's solution, the dynamic action of the water on the dam can be visualized as that of a certain body of water moving together with the dam while the remainder of the reservoir remains effectively stationary. The body of water moving with the dam may be imagined as effectively having frozen into horizontal layers of ice, with the remainder of the reservoir being emptied. The layers of ice are considered to support one another by vertical forces only, with no shear force in between. The layers are attached firmly to the dam so that the dam will exert the horizontal forces necessary to move them back and forth as it oscillates. Therefore, the forces exerted on the up-stream face of the dam can be represented as inertia forces similar to those due to the moving mass of the dam itself.

The shape of the body of water considered to be moving in concert with the dam needs to be determined to evaluate the inertia forces which correspond to the pressure exerted by the water due to dynamic action. According to Westergaard, it can be assumed that this body is defined by a parabolic shape as described by the following expression (Figure 9) :

$$b = \frac{7}{8}\sqrt{hy} \quad \dots\dots\dots\dots \quad (6)$$

with a maximum dimension of 7/8 h at the base, where h is the height of water column above the base of the reservoir and b is as defined in Figure 9.

The hydrodynamic pressure, p, at a depth y is given by the following :

$$p = \frac{7}{8}\sqrt{hy}\, K_h \gamma_w. \quad \dots\dots\dots\dots \quad (7)$$

where γ_w = unit weight of water = ρ_w g

ρ_w = density of water

The total hydrodynamic force, F_{dyn}, is obtained by integrating the pressure over the height of the dam as follows :

$$F_{dyn} = \int_o^h p\,dy = \frac{7}{12} h^2 K_h \gamma_w \quad \ldots\ldots\ldots\ldots\ldots \quad (8)$$

The resultant water force acts at a height of 0.4 h above the base of the reservoir.

It should be noted that only horizontal shaking was considered but any vertical acceleration can be accounted for by factoring up the unit weight of water by the ratio $(1+K_v)$. The tilting principle as discussed in Section 2.2.2 cannot be applied to water.

It should be noted that the solution by Westergaard (1933) represents an approximation, which is generally on the safe side, i.e. the hydrodynamic pressure acting on the wall will be over-estimated. More exact solutions were derived by Werner & Sundquist (1949) and Bustamante & Flores (1966) which also cover the situations where the dams have a sloping face. These latter solutions are summarised in Figure 10.

3.2.2 Hydrodynamic Pressure in Soil

Matsuo & O-Hara (1965) proposed a model for estimating the dynamic pore water pressure of saturated sand during earthquake shaking. The main assumptions of this method are that the soil skeleton undergoes no deformation during vibration, that water flows through the pores in the soil, and that the Navier-Stokes equations apply.

Given the equation of continuity and the equation of characteristics, and assuming Darcy's law and appropriate boundary conditions, the force due to dynamic pore water pressure and its point of action can be obtained for the steady state under continuous shaking. The dynamic forces given by these solutions are summarised in Figure 8. The point of action can be taken as 0.4 H above the base of the wall, where H is the wall height.

It should be noted that the dynamic force depends on the period of vibration (T_p), magnitude of acceleration, permeability of the soil (k_s), bulk modulus of water (K_w), etc. For example, if H = 7m, porosity n = 0.5, k_s = 10^{-4}m/sec, T_p = 2 sec and K_w = 2.04 x 10^6 kN/m^2, then

$$\frac{\rho_w n g w H^2}{k_s K_w} = 3.77 \quad \ldots\ldots\ldots\ldots\ldots\ldots\ldots \quad (9)$$

and the dynamic force, P, is equal to 0.34 $\gamma_w K_h H^2$.

When the pore size and the permeability are very large, the solutions given in Figure 8 will tend towards Westergaard's solution. On the other hand, if the permeability is very small, the hydrodynamic pressure will tend to become zero. The solution appears to agree with laboratory results for these two limiting cases.

As the Matsuo & O-Hara model assumes an incompressible soil skeleton, it is not strictly applicable when the factor of safety is low, or where large soil deformation is likely. Nevertheless, for a soil skeleton with very low compressibility and high permeability (e.g. rockfill) where the water will behave as free water, this model will give an insight into the dominant mechanism and magnitude of the likely pore pressure build-up.

A generalised approach has been put forward by Matsuzawa et al (1985) for computing the components of dynamic earth pressure and hydrodynamic pressure of submerged soils. This method unifies a modified version of the Mononobe-Okabe method, Matsuo & O-Hara's solutions and Westergaard's solution. However, it should be noted that the simplified equations derived by Matsuzawa et al (1985) only apply to simple geometries, such as where the groundwater table is at ground level. In principle, the use of the trial wedge method with allowance for dynamic water pressures as appropriate will be more versatile for general application.

3.3 Dynamic Pore Water Pressure Due to Deformation of Soil Skeleton

3.3.1 Sarma's (1975) Approach

Because of the acceleration of soil particles and water, the soil skeleton may deform which can result in an increase or decrease in volume. The shear and/or volumetric deformation will in turn cause a corresponding change in the dynamic pore water pressure, and hence the effective stress of the soil.

Sarma (1975) proposed a method for estimating the dynamic pore water pressure generated during earthquakes for an effective stress analysis. A summary of this method is given in Appendix A. In this approach, the dynamic pore water pressure is assumed to be generated by shear deformation of soil under undrained conditions, and therefore the dynamic viscosity and permeability of the soil can be ignored. Skempton's pore pressure coefficients A and B are used to estimate the excess pore pressure (Δu) at limiting equilibrium, as follows :

$$\Delta u = B[\Delta\sigma_3 + A(\Delta\sigma_1 - \Delta\sigma_3)] \quad \cdots\cdots\cdots\cdots\cdots \quad (10)$$

where $\Delta\sigma_1$ = change in major principal stress
$\Delta\sigma_3$ = change in minor principal stress

It should be noted that Sarma's approach only considers the changes in the magnitude, but not the directions, of the principal stresses. For the calculation of Δu, the principal stresses σ_1 and σ_3 before the earthquake shaking must be known. However, the Mohr's circle of stresses is strictly indeterminate at this stage. An assumption therefore needs to be made that the state of stress at any point along the potential slip plane will be the same as if with an angle of shearing resistance of ϕ' being equal to ψ, where $\psi = \tan^{-1}(\tan\phi'/F)$ and F is the partial factor of safety against sliding as described below.

With the above assumption, it becomes possible to draw the Mohr's circle which passes through the point σ_n' and τ (where σ_n' is the normal stress and τ is the shear stress), and will be tangential to the factored strength envelope inclined at an angle ψ. Given the stress fields before and during earthquake loading, the excess pore water pressure can be determined using Equation 10. Sarma's method considers pore water pressure generation due to shear deformation of the soil skeleton, which is not considered in the theory by Matsuo and O-Hara (1965).

The proposed procedure for seismic analysis of gravity retaining wall using the trial wedge method with allowance for dynamic pore water pressure is shown in Figure 11. For a particular sliding wedge, say, that defined by AB2, limiting equilibrium is assumed for surfaces A2, AB and OA when both tan ϕ' and tan δ_b are factored by a static partial factor of safety, F_2. Accordingly, the reaction, R_2, at the sliding surface A2 and hence the average normal stress and shear stress can be determined. With Sarma's assumptions, the Mohr's circle of stresses can be drawn and the principal stresses (i.e. σ_{10}, σ_{30}) determined. When seismic loading is applied, excess pore water pressure (Δu) will be generated over the saturated portion of the sliding surface A2 due to shearing.

In principle, dynamic pore water pressures may be determined using this method if large shear deformation is anticipated. Principal stresses, σ_{1d} & σ_{3d}, and Δu are related by Equation 10, and the new factor of safety under dynamic conditions (i.e. F_{2d}) can be calculated. The same procedure is repeated for other sliding surfaces such as A1, A2, A3, and the minimum factor of safety can therefore be obtained during earthquake loading (Figure 11). It is important to note that the critical slip surface under earthquake loading (i.e. the one with minimum factor of safety) may be different from that of static condition.

For practical purposes, it is suggested that Δu may be assumed to be zero along the back and base of the wall because significant relative deformation is not expected along these interfaces compared to that along the sliding surface, the usual presence of a drainage layer at the wall back, and that the wall base is a relatively short plane of action.

It should be noted that the validity of the above approach depends on the following factors :

(a) Whether the stresses in the soil along the sliding plane can be predicted accurately. While the limiting equilibrium method can provide satisfactory results for stability analysis, the stress states predicted from this method may be doubtful. Furthermore, the soil behind a retaining wall is conventionally assumed to reach the active state (i.e. a factor of safety of unity for the backfill), but Sarma's approach assumes that the backfill and the founding material have the same partial factor of safety.

(b) Whether the appropriate pore pressure parameter A can be determined. The A value should be determined under the appropriate stress path. However, this is not done in conventional laboratory tests in Hong Kong.

An example of the above approach is given in Figure 12. In this example, A values of zero and 0.8 have been considered respectively. It is assumed that the excess pore pressure is generated only on the submerged portion of the backfill.

The results summarised in Figure 12 show that the minimum static partial FOS against sliding is 1.4. For $K_h = 0.08$ and $K_v = 0$, the minimum FOS is calculated to drop to 1.16 and 1.14 for A = 0 and A = 0.8 respectively for a groundwater table 3 m above the wall base. The induced excess pore water pressure does not appear to be significant and the result seems relatively insensitive to the A value assumed. The results suggest that if the permanent groundwater table is not high and the A value is relatively small, the generation of excess pore water pressure may be ignored in practice. Where the water table is high or where the thickness of saturated soil is large, the excess pore water pressure will be more sensitive to the A value of the soil, and may need to be considered in design.

3.3.2 Liquefaction of Loose Backfill

If the backfill is submerged and is very loose, it may liquefy upon seismic excitation. Under such circumstances, Pappin (1992) suggests that the active force per unit length of wall, P_{AL}, will be equal to that of a fluid with a density of the soil-water suspension (γ_l) as follows :

$$P_{AL} = 0.5\ \gamma_l\ H^2 \quad \ldots\ldots\ldots\ldots\ldots\ldots\ldots \quad (11)$$

where γ_l = saturated unit weight of soil

This represents a possible extreme state for existing walls in Hong Kong retaining loose fill which have not been designed to current geotechnical standards. Pun (1992) has reviewed the published correlations of the liquefaction potential but it should be noted that this work relates principally to level ground situations.

A more rational approach to assessing the vulnerability to liquefaction would be to investigate the shear behaviour of the loose material under cyclic loading and determining the corresponding A value at failure. Alternatively, the undrained shear strength of the material at a given density and confining stress may be related to a given number of cycles of excitation (which can be correlated to the magnitude of the design earthquake). Once a better understanding of the material behaviour is available, the susceptibility of the material to liquefaction can be correlated with its insitu state by means of density or penetration resistance, and the stability of the retaining wall can be evaluated. More work is required in this area.

3.4 Recommended Approach

3.4.1 Free Standing Water

The hydrodynamic pressure may be determined using the approximate solution by Westergaard (1933) which is generally conservative (Section 3.2.1). Alternatively, the solutions given in Figure 10 may be used. The latter solutions cover the situation of a dam with a sloping back.

3.4.2 Highly Permeable Material

For wall retaining highly permeable coarse backfill, such as rockfill, the principal mechanism of generation of dynamic pore water pressure is associated with water movement through the interstices of the soil. In this situation, the Matsuo & O-Hara's approach (Section 3.2.2) may be adopted. The deformation of this category of backfill is generally so insignificant that it can be ignored in estimating the dynamic pore water pressure.

3.4.3 Moderate- to Low-permeability Material

For this category of material, the principal mechanism of generation of dynamic pore water pressure is due to deformation of the soil skeleton under seismic loading.

(1) Material with a low pore pressure parameter 'A' value For properly re-compacted material or dense soils, the A value is likely to be low. Also, significant accumulation of pore water pressure is unlikely as prolonged shaking is not envisaged in areas of low seismicity, such as Hong Kong. In this case, it is generally not necessary to consider the effects of dynamic pore water pressure in the design.

(2) Material with a large pore pressure parameter 'A' value For strongly contractive, moderate- to low-permeability backfill that has a tendency to produce positive pore water pressure during shearing, i.e. degradable soils with a large A value (Wong & Pang, 1992), Sarma's method (Section 3.3.1) can, in principle, be used to estimate the dynamic pore water pressure. This method involves fairly complex calculations and an assessment of the appropriate A value under dynamic loading. In Hong Kong, the A value is seldom determined under the appropriate anisotropic conditions and relevant stress paths. Thus, the validity of the results may be questionable. In view of this, the more complicated and rigorous analysis proposed by Sarma (1975) may not be justified.

For practical purposes, it is suggested that a simplified approach may be adopted in the absence of high quality data from sophisticated stress path tests under cyclic loading. As a first approximation, it is suggested that the Δu generated in the conventional isotropically consolidated undrained triaxial compression tests at the appropriate stress levels can be used as a reference for the likely dynamic pore water pressure. With the Δu estimated approximately, the seismic analysis of a retaining wall can then be carried out in the normal manner using the Mononobe-Okabe method or the trial wedge method as appropriate. The above suggested methodology is obviously a fairly coarse approximation but this pragmatic approach is considered sufficient for practical purposes. If the approximate assessment suggests that the design may be critically dependent on the dynamic pore water pressure response, consideration should be given to carrying out cyclic load tests, as appropriate.

3.4.4 Liquefiable Loose Fill

For a saturated loose backfill where there is a possibility of significant build up of excess pore pressure due to cumulative strains, caution must be exercised in assessing whether liquefaction (i.e. shear strength approaching zero due to large increase in positive pore water pressure) may occur. In this case, more sophisticated testing to evaluate the dynamic properties of the material may need to be considered.

Reference may be made to Pun (1992) for background discussion of the range of methods for assessing the liquefaction potential.

4. ASSESSMENT OF STABILITY AND DISPLACEMENT OF RETAINING WALLS

4.1 Stability of Retaining Wall under Seismic Loading

There are three different modes of instabilities, namely sliding, overturning and bearing capacity failure, which should be checked.

The procedure for computing the dynamic factors of safety against sliding and overturning is same as that for static calculations, except that the inertia of the gravity wall itself must also be included when earthquake loading is considered.

In calculating the dynamic bearing capacity, the effect of shaking on the foundation material must be considered. A simplified approach is to rotate the ground by an angle θ, where $\theta = \tan^{-1}(K_h)$ if K_v is taken as zero (Figure 13), with the application of appropriate correction factors for sloping ground. It should be noted that when the ground is effectively rotated, the wall will tilt away from the slope face by an angle Ω (Figure 13(b)), but there are no published correction factors for such tilting. As this effect is beneficial and that the tilt angle is generally small, the tilting of the wall can be conservatively ignored. Therefore, as a first approximation, the wall may be analysed as if it were founded on level ground adjacent to a slope with an angle Ω to the horizontal as shown in Figure 13(c).

When the disturbing force to a retaining wall exceeds the restoring force (i.e. factor of safety below unity), the wall will move under a net disturbing force. A number of authors (e.g. Newmark, 1965; Sarma, 1975; Seed, 1979) pointed out that in the design of geotechnical structures for earthquake loading, the consideration of deformation may be more appropriate than the factor of safety on the shear strength because seismic loading is a transient effect. Provided that the material and overall soil-structure system is ductile, a factor of safety of less than unity may be acceptable under seismic loading if the deformation is tolerable.

There are two main modes of deformations for a gravity retaining wall, namely lateral displacement and rotation. The former is due to inadequate sliding resistance, whilst the outward tilting of a wall may be caused by inadequate resistance to overturning and/or bearing. The methods of assessing the two modes of deformation are given in the following sections.

4.2 Lateral Displacement of Retaining Wall under Seismic Loading

A range of models with different assumptions have been proposed to estimate displacements. However, the sliding block model is generally considered the most appropriate method for routine analysis.

The sliding block model was first proposed by Newmark (1965) for estimating the dynamic wall displacements. By computing the ground acceleration at which movement starts to begin (i.e. when the critical acceleration coefficient, K_c, is exceeded) and by summing up the displacements during the period of instability, the final cumulative displacement of the sliding mass can be evaluated. The calculation is based on the assumption that the material is rigid-plastic and the moving mass is displaced as a single rigid body with resistance mobilized along a sliding surface. The concept of the sliding block model is shown in Figure 14.

Based on the sliding block concept, Sarma (1975) derived solutions for a rectangular pulse, a triangular pulse, and a half sine pulse respectively (Figure 15). The results have been shown to bracket the observations made in actual earthquakes reasonably well. Sarma also used a number of acceleration records, as indicated on Figure 15, to produce the following empirical equation as an upper-bound estimate of the displacement where the nature of the strong motion is uncertain :

$$\log\left[\frac{1}{C}\,\frac{4x_m}{gK_mT^2}\right] = 1.07 - 3.83\frac{K_c}{K_m} \quad \ldots\ldots\ldots\ldots\ (12)$$

where x_m = maximum displacement of sliding block
K_m = design ground acceleration coefficient
C = $\cos(\beta' + \theta' - \phi')/\cos\phi'$ if K_v is acting upwards
= $\cos(\beta' - \theta' - \phi')/\cos\phi'$ if K_v is acting downwards
= $\cos(\beta' - \phi')/\cos\phi'$ if K_v is zero
K_v = vertical ground acceleration coefficient
β' = inclination of equivalent sliding plane to horizontal
θ' = inclination of resultant inertia force to horizontal
ϕ' = angle of shearing resistance of soil
T = predominant half period of the ground motion in seconds

Ambraseys and Menu (1988) related the dynamic ground displacements to the ratio of critical acceleration to design acceleration (i.e. K_c/K_m) based on a large number of ground motion records obtained at a source distance of less than half that of the source dimensions. A method was proposed to assess the likelihood of exceeding the predicted displacements for the near-field earthquakes with a magnitude ranging from 6.6 to 7.3 for both level ground and sloping ground (Figure 16). The underlying assumption of this method is that the resistance to sliding remains constant and equal to that mobilised at limiting equilibrium.

It should be noted that the records considered by Ambraseys & Menu are all near-field events, with most of the monitoring stations being situated less than 10 km from the epicentres. Hong Kong can also be susceptible to more distant earthquakes with a much larger epicentral distance, hence deviations from Ambraseys & Menu's solutions may be expected. There are as yet no strong motion records in Hong Kong and hence the derivation of similar graphs for more distant earthquakes is not possible. However, it is generally expected that the relationship between displacement and K_c/K_m would lie within a narrow range. It is therefore suggested that either Ambraseys and Menu's (1988) chart or Sarma's (1975) solutions can be used for assessing the likely sliding displacements for practical purposes.

An example of the use of the sliding block theory to estimate the displacement of a typical retaining wall in Hong Kong is shown in Figure 17. The wall is 8 m high and 1.9 m wide, retaining a dry cohesionless backfill with a ϕ' value of 35°. The friction angles at the back and the base of the wall are 17.5° and 30° respectively. The static factor of safety against sliding is calculated to be 1.58, with the critical sliding surface inclined at about 61° to the horizontal. The critical acceleration coefficient is 0.13, and the associated sliding surface shifts to an angle of 53° to the horizontal.

Now, if an earthquake with a peak acceleration K_m of 0.2 is exerted on the wall, the acceleration ratio K_c/K_m will be 0.65. From Ambraseys & Menu's graph shown in Figure 16, the estimated displacement is about 8.5 mm for 50% probability of exceedance.

By way of comparison, the displacement is also estimated using Sarma's solution. In this approach, the normal and shear forces on the sliding planes have to be determined in order to calculate the equivalent angle β' of the sliding plane (Figure 17). Moreover, the characteristics of the earthquake records (e.g. predominant half period, T) are also required. Based on Figure 15, the calculated displacements are about 6.4 mm, 1.4 mm and 0.5 mm for a rectangular, half sine and triangular pulse respectively if T is taken to be 0.2 sec. On the other hand, if Equation 12 is used, a displacement of 0.9 mm is calculated. For near-field earthquakes, T is typically around 0.2 second whereas for far-field earthquakes, T is usually in the range of 0.5 to 1 second. If local strong motion records become available in future, the more appropriate value of T may be used for analysis.

The above simple example seems to indicate that the Ambraseys & Menu's solutions give a slightly higher predicted displacement as that of Sarma's method. The comparison is not strictly rigorous because the probability of exceedance is not considered in Sarma's solution. In practice, Ambraseys & Menu's solution has the obvious advantage of being simple as the solutions only depend on the acceleration ratio K_c/K_m, whereas Sarma's solutions require the calculation of the C parameter (Figure 15) which is quite a tedious procedure.

4.3 Rotation of Wall under Seismic Loading

The rotation of a retaining wall can be caused by one of the following failure mechanisms :

(a) Overturning Instability - This mode of rotation about the wall toe will occur when the overturning moment exceeds the restoring moment.

(b) Bearing Instability - This mode of rotation about the wall heel will occur when the bearing capacity of the founding material is exceeded.

When seismic loading is exerted on a retaining wall, both the overturning moment and the bearing pressure will increase. When the overturning moment becomes close to the restoring moment, very high and concentrated bearing pressure will be generated near the wall heel. Therefore, unless the founding material is very strong (e.g. moderately decomposed rock or better), the wall will tend to rotate about the heel due to inadequate bearing capacity.

For founding materials such as completely or highly decomposed rock, bearing instability may be the predominant mode of movement. On the other hand, if the wall is founded on rock in which case bearing will not be a problem, overturning instability can become predominant.

Once net outward tilting occurs, the wall cannot be restored to its original position due to the much larger passive resistance that has to be overcome in doing so. Progressive rotation can lead to a catastrophic wall failure if the cumulative rotation is excessive. Therefore, wall rotations must not be ignored in design consideration. Unlike displacement assessment, there is generally little literature on rational methods of estimating the wall rotation.

In light of the above considerations, a simplified method that has been formulated from basic dynamic equations is proposed, with the following assumptions :

(a) The total dynamic earth pressure and its points of action remain unchanged before and after the wall rotates. In practice, the downward acceleration of the soil wedge as the wall moves away from the retained material will reduce the force that is exerted on the wall.

(b) The lever arms of all the forces on the wall remain constant regardless of the rotation. This assumption may not be justified if the rotation becomes too large.

(c) The resultant normal force at the base and its eccentricity maintain the same values as that at K_c for rotation about the heel due to inadequate bearing capacity when the Kc for bearing failure is exceeded.

(d) The horizontal seismic coefficient, C_{AE}, is linearly proportional to the ground acceleration coefficient K_h. As shown in Figures 3 to 5, this assumption is valid up to a K_h of about 0.2.

The equation for angular acceleration is:

$$\ddot{\theta} = M_o/I \qquad \text{(13)}$$

where $\ddot{\theta}$ = angular acceleration
M_o = net moment (i.e. disturbing moment minus restoring moment)
I = moment of inertia of the wall

It should be noted that the moment is taken about the toe and the heel of the wall for overturning instability and bearing instability respectively.

With the above assumptions, the value of $\ddot{\Theta}$ is given by the following :

$$\ddot{\Theta} = D\,(K_h - K_c) \quad \ldots\ldots\ldots\ldots\ldots\ldots\ldots \quad (14)$$

where D is a constant as defined below.

For overturning instability,

$$D = [\tfrac{1}{2}\,\gamma\,H^2\,\mu\,(h_2 \cos\delta - B \sin\delta) + W\,H/2]/I \quad \ldots\ldots\ldots \quad (15)$$

and for bearing instability,

$$D = [\tfrac{1}{2}\,\gamma\,H^2\,\mu\,(h_2 \cos\delta) + W\,H/2]/I \quad \ldots\ldots\ldots\ldots \quad (16)$$

where h_2 = height of the point of action of dynamic force above the wall base.

μ = gradient of C_{AE} versus K_h plot (see Section 2.2.2)

C_{AE} = horizontal seismic coefficient

B = width of the wall

The derivation of the above formulation is given in Appendix B.

This is similar to the basic equation for the assessment of displacement as proposed by Sarma (1975), namely,

$$a = C\,g(K_h - K_c) \quad \ldots\ldots\ldots\ldots\ldots\ldots\ldots \quad (17)$$

where a = acceleration of the sliding mass

It is evident that Equations 14 and 17 have the same form, with $\ddot{\Theta}$ and D replaced by a and the term "C g" respectively. As Sarma has produced solutions for Equation 14 for different types of seismic wave based on actual acceleration records (Figure 15) in terms of the dimensionless displacement $4\,x_m/(C\,g\,K_m\,T^2)$, the same solution can be used to give angular displacement by substituting the term "C g" with D.

It should be noted that the above proposed method for estimating the dynamic wall rotation is approximate but it is considered adequate for a rough assessment of the order of rotation.

4.4 Discussion

There are other methods put forward in the literature for assessing the movement of a retaining wall under seismic loading. For instance, the method suggested by Richards & Elms (1979) is used as the basis for the design of bridge abutments in California (ATC, 1981). In this method, the permanent slip is determined in terms of the peak acceleration and peak velocity of the sliding plane, together with the maximum acceleration that can be transmitted across the block/plane interface without slippage occurring. Furthermore, an explicit procedure was put forward for selecting the design acceleration coefficient based on the concept of allowable permanent movement.

Nadim & Whitman (1993) analysed the sliding of rigid walls by means of finite element methods. They found that the mechanism can be quite complicated owing to the deformability of the backfill. They recommended the computation of the natural frequency of the backfill, f_1, as follows :

$$f_1 = V_s/4h \quad \quad (18)$$

where V_s = the shear wave velocity of the backfill
h = height of the backfill

Suggestions were made by Nadim & Whitman concerning whether amplification effects need to be allowed for in Richards & Elms' analysis, as a function of the ratio f/f_1, where f is the predominant frequency of the earthquake motion.

Richards & Elms' method has been specifically developed for bridge abutments where movements can be critical. Although being more complicated, this method may constitute a suitable alternative basis for assessing wall displacement to that suggested by Sarma (1975) and by Ambraseys and Menu (1988).

Tilting of retaining walls has received relatively little attention. Some notable studies include the investigation of coupled sliding and tilting during earthquakes by Nadim & Whitman (1984) using numerical methods. This is generally of research nature but one of the key findings is that the dominant deformation pattern is likely to be either pure sliding or pure tilting, with coupled modes of permanent deformations being very rare. Tilting of walls under dynamic conditions has also been studied by Anderson et al (1987) using centrifuge testing.

Al-Homoud & Whitman (1992) studied the tilting of gravity walls during earthquakes using finite element method, and a fairly complicated methodology is suggested for evaluating the permanent outward tilt.

Having reviewed the currently available methods, it is considered that the simplified method of assessing the tilt put forward in Section 4.3 is sufficient for practical purposes.

5. RECOMMENDED PROCEDURE FOR SEISMIC ANALYSIS OF RETAINING WALLS

5.1 Recommended Procedure of Analysis

The available literature on seismic design of gravity retaining walls have been critically reviewed. The appropriate methods of assessing the dynamic earth pressure and dynamic pore water pressure for practical purposes have been considered. In addition, a new method of evaluating the permanent tilt of a wall has been developed for practical purposes.

The following is a summary of the recommended procedure for the analysis of concrete gravity-type retaining walls subjected to earthquake loading :

(a) The pseudo-static method should be adopted for estimating the dynamic earth pressure using the Mononobe-Okabe formula or the trial wedge method, as appropriate (Sections 2.2.2 and 2.2.3).

(b) The dynamic pressure increment should be conservatively assumed to lie at $^2/_3$ H above the base of the wall (Section 2.2.6).

(c) The wall inertia should be taken into account (Section 2.2.1).

(d) The Westergaard's solution or the solutions summarised in Figure 10 (Section 3.2.1) should be used for calculating the hydrodynamic pressure on a wall arising from free-standing water.

(e) For typical dense backfill with a low pore pressure coefficient A, no dynamic excess pore water pressure need to be allowed for in the analysis (Section 3.4.3).

(f) If a substantial portion of the backfill is under submerged condition and the soil is highly "degradable" (i.e. generation of positive excess pore pressure upon shearing) with a high A value, it is recommended that Sarma's (1975) approach as outlined in Section 3.3.1 may reasonably be adopted to determine for the development of excess pore water pressure under seismic condition. For practical purposes, the excess pore water pressure along the back and base of the wall may be ignored.

(g) Given the estimated total dynamic earth pressure under earthquake loading, the factors of safety against sliding, overturning and bearing failure may be calculated.

(h) If the factor of safety for any mode of instability is below unity, the corresponding critical acceleration (K_c) should be determined. This would then permit an evaluation of the associated deformation, e.g. displacement due to sliding instability or wall rotation due to overturning or bearing instability, as appropriate (Sections 4.2 and 4.3). Unfactored shear strength parameters should be used for deformation assessment.

5.2 Examples of Analysis

Two examples of seismic analysis of gravity retaining walls are given in the following to illustrate the calculation of displacements under dynamic condition. The first example considers a wall founded on rock whilst the second case involves a wall founded on soil.

5.2.1 Case 1

The problem, together with the results of analysis, are shown in Figure 18. The concrete wall is 8 m high and 2.1 m wide, with a unit weight of 24 kN/m^3. The backfill has strength parameters of c' = 0 and ϕ' = 35°. The wall friction and the base friction are taken to be 17.5° and 35° respectively for the purposes of this example.

As the wall is assumed to be founded on rock, bearing instability will not be a problem. Under static conditions, the wall has partial factors of at least 1.2 on the soil shear strength and the base friction against sliding and overturning respectively. The partial safety factor is that defined in Geoguide 1 (GEO, 1993). Therefore, the wall satisfies the minimum requirements of Geoguide 1.

When seismic loading corresponding to a K_h value of 0.25 (i.e. 25% g) is applied, the safety factors against overturning and sliding will drop below unity on the basis of unfactored strength. This means that the wall will deform under the out-of-balance loads. Therefore, the critical seismic coefficients (K_c) for overturning and sliding will need to be determined, and these are found to be 0.04 and 0.22 respectively.

Equation 12 and the assumption of T = 0.2 sec have been used for rotation assessment, and Figure 16 has been used for displacement assessment. There is no horizontal movement up to K_h = 0.22. With K_h = 0.22, the K_c for overturning is exceeded and the estimated rotation is only 1.15°, or about 161 mm horizontal displacement at the top of the wall. When K_h equals 0.25, both the K_c for sliding and overturning are exceeded, and the estimated displacement and rotation are 1.6 mm and 1.42° (which corresponds to 199 mm displacement at the top) respectively. The mode of deformation is shown in Figure 18.

Thus, it can be seen from this example that the dominant mode of movement of the wall corresponds to overturning, whereas translational movements are unlikely to be significant for the assumptions made for the base friction.

5.2.2 Case 2

The problem and the analysis results are shown in Figure 19. The wall is 8 m high and 3.1 m thick. The backfill has shear strength parameters of c' = 0 and ϕ' = 36°. The wall friction and base friction are taken as 18° and 33° respectively for the purpose of this example. The wall is founded on a soil with c' equals zero and ϕ' = 38°. Under static conditions, the wall has partial safety factors on shear strengths and base friction of at least 1.2 against sliding, overturning and bearing failure. Hence, the wall satisfies the requirements of Geoguide 1 (GEO, 1993).

The K_c value for bearing failure is calculated to be 0.062. The K_c values for sliding and overturning are larger than 0.15, and therefore when $K_h = 0.15$, the predominant mode of movement will be rotation about the heel. The estimated rotation is 0.082°, which corresponds to a displacement of 11.4 mm at the top of the wall. The mode of deformation is shown in Figure 19.

6. CONCLUSIONS

Based on a critical review of the currently available methods for assessing seismic stability of gravity retaining walls, it is considered that the pseudo-static analysis is most appropriate for the routine analysis for typical concrete gravity-type retaining walls in Hong Kong. The Mononobe-Okabe method or the trial wedge method can be used to calculate the seismic forces induced on a retaining wall.

Where the factor of safety under dynamic condition is less than unity, the resulting displacement must be determined. Methods of assessing the dynamic displacement of a wall have been reviewed. It is recommended that the method by Ambraseys & Menu (1988) and that by Sarma (1975) may be used in practice. A new simplified method for assessing the rotation of a retaining wall has been proposed as summarised in Section 4.3.

More advanced methods, such as dynamic response analysis and finite element method, are capable of allowing for the dynamic characteristics of the soil-structure system. However, these advanced methods are usually not justified for the analysis of conventional gravity retaining walls subjected to earthquake loading, and the above simple methods are generally adequate.

7. REFERENCES

Aggour, M. & Brown, C. (1979). Evaluation of methods used in the determination of dynamic earth pressure. Proceedings of the Second South Pacific Regional Conference on Earthquake Engineering, vol. 2, pp 313-323.

Al-Homoud, A. & Whitman, R.V. (1992). Evaluating tilt of gravity retaining walls during earthquakes. Proceedings of the Tenth World Conference on Earthquake Engineering, vol. 3, pp 1683-1688.

Ambraseys, N.N. & Menu, J.M. (1988). Earthquake-induced ground displacement. Earthquake Engineering and Structural Dynamics, vol.16, pp 985-1006.

Ambraseys, N.N. and Sarma, S.K. (1967). The response of earth dams to strong motion. Geotechnique, vol. 17, pp 181-213.

Anderson, G.R., Whitman, R.V. & Germaine, J.T. (1987). Tilting Response of Centrifuge-Modeled Gravity Retaining Wall to Seismic Shaking : Description of Tests and Initial Analysis of Results. Report No. R87-14, Department of Civil Engineering, MIT, Cambridge, Mass. (Unpublished).

ATC (1981). Seismic Design Guidelines for Highway Bridges. Applied Technology Council, Report No. ATC-6, Palo Alto, California.

Au Yeung, Y.S. (1992). Evaluation of Seismic Stability of Retaining Walls in Hong Kong. MSc Dissertation, Department of Civil Engineering, Imperial College of Science, Technology & Medicine, University of London, 92 p. (Unpublished).

Bustamante, J.I. & Flores, A. (1966). Water pressure on dams subjected to earthquakes. Journal of the Engineering Mechanics Division, Proceedings of the American Society of Civil Engineers, vol. 92, no. EM5, pp 115-126.

Byrne, P.M. & Salgado, F. (1981). Seismic response of retaining structures. Proceedings of the International Conference on Recent Advance in Geotechnics, Earthquake Engineering and Soil Dynamics, pp 727-732.

Dorwick, D.J. (1987). Earthquake Resistant Design. (Second edition). John Wiley & Sons, 519 p.

GEO (1993). Guide to Retaining Wall Design (Geoguide 1). (Second edition). Geotechnical Engineering Office, Hong Kong Government, 267 p.

Highways Department (1993). Structures Design Manual for Highways and Railways. Highways Department, Hong Kong Government, 210 p.

Matsuo, H. & O-Hara, S. (1965). Dynamic pore water pressure acting on quay walls during earthquakes. Proceedings of the Third World Conference on Earthquake Engineering, New Zealand, pp 130-140.

Matsuzawa, H., Ishibashi, I. & Kawamura, M. (1985). Dynamic soil and water pressures of submerged soils. Journal of Geotechnical Engineering, American Society of Civil Engineers, vol. 111, pp 1161-1176.

Mononobe, N. & Matsuo, H. (1929). On the determination of earth pressures during earthquakes. Proceedings of World Engineering Congress, vol. 9, pp 177-185.

Nadim, F. & Whitman, R.V. (1984). Coupled sliding and tilting of gravity retaining walls during earthquakes. Proceedings of the Eighth World Conference on Earthquake Engineering, San Francisco, vol. 3, pp 477-484.

Nadim, F. & Whitman, R.V. (1993). Seismic analysis and design of retaining walls. Norwegian Geotechnical Institute Publication No. 190, 26 p.

Newmark, N.M. (1965). Effects of earthquake on dams and embankments. Geotechnique, vol. 15, pp 129-160.

Okabe, S. (1926). General theory of earth pressure. Journal of Japanese Society of Civil Engineer, vol. 2.

Pappin, J.W. (1992). Design of Foundations and Soil Structures for Seismic Loading. Contribution to Chapter 7 in the Publication on cyclic loading of soils, edited by M O'Reilly & S. Brown, pp 306-366.

Prakash, S. & Nandkuamaran, P. (1973). Dynamic earth pressure distribution on rigid walls. Proceedings of Symposium on Earth and Earth Structures Subjected to Earthquakes and Other Dynamic Loads, Roorkee, vol. 1, pp 11-16.

Pun, W.K. (1992). Earthquake Resistance of Buildings and Marine Reclamation Fills in Hong Kong. Geotechnical Engineering Office, Hong Kong Government, 55 p. (GEO Report No. 16)

Pun, W.K. & Ambraseys, N.N. (1992). Earthquake data review and seismic hazard analysis for the Hong Kong region. International Journal of Earthquake Engineering and Structural Dynamics, vol. 21, pp 433-443.

Richards, R. Jr. & Elms, D. (1979). Seismic behaviour of gravity retaining walls. Journal of Geotechnical Engineering, American Society of Civil Engineers, vol. 105, pp 449-464.

Sarma, S.K. (1975). Seismic stability of earth dams and embankments. Geotechnique, vol.25, pp 743-761.

Seed, H.B. (1979). Consideration in the earthquake-resistant design of earth and rockfill dams. Geotechnique, vol. 29, pp 215-263.

Stamatopoulos, C. & Whitman, R.V. (1990). Prediction of permanent tilt of gravity retaining walls by the residual strain method. Proceedings of the Fourth US National Conference on Earthquake Engineering, Palm Springs, California, vol. 3, pp 683-692.

Steedman, R.S. (1984). Modelling the Behaviour of Retaining Walls in Earthquakes. PhD thesis, Engineering Department, Cambridge University, 198 p. (Unpublished).

Steedman, R.S. & Zeng, X. (1990). The influence of phase on the calculation of pseudo-static earth pressure on a retaining wall. Geotechnique, vol. 40, pp 103-112.

Werner, P.W. & Sundquist, K.J. (1949). On hydrodynamic earthquake effects. Transactions, American Geophysical Union, vol. 30, no. 5, pp 636-646.

Westergaard, H.M. (1933). Water pressures on dams during earthquakes. Transactions of the American Society of Civil Engineers, Paper no. 1835, pp 418-433.

Wong, H.N. (1991). Evaluation of Seismic Stability of Slopes in Hong Kong. MSc Dissertation, Department of Civil Engineering, Imperial College of Science, Technology & Medicine, University of London, 113 p. (Unpublished).

Wong, H.N. & Li, A.C.O. (1994). Dynamic Analysis of the Stability of Cantilevered Retaining Wall Subjected to Earthquake Loading. Geotechnical Engineering Office, Hong Kong Government. (In preparation).

Wong, H.N. & Pang, P.L.R. (1992). Assessment of Stability of Slopes Subjected to Blasting Vibration. Geotechnical Engineering Office, Hong Kong Government, 119 p. (GEO Report No. 15).

LIST OF FIGURES

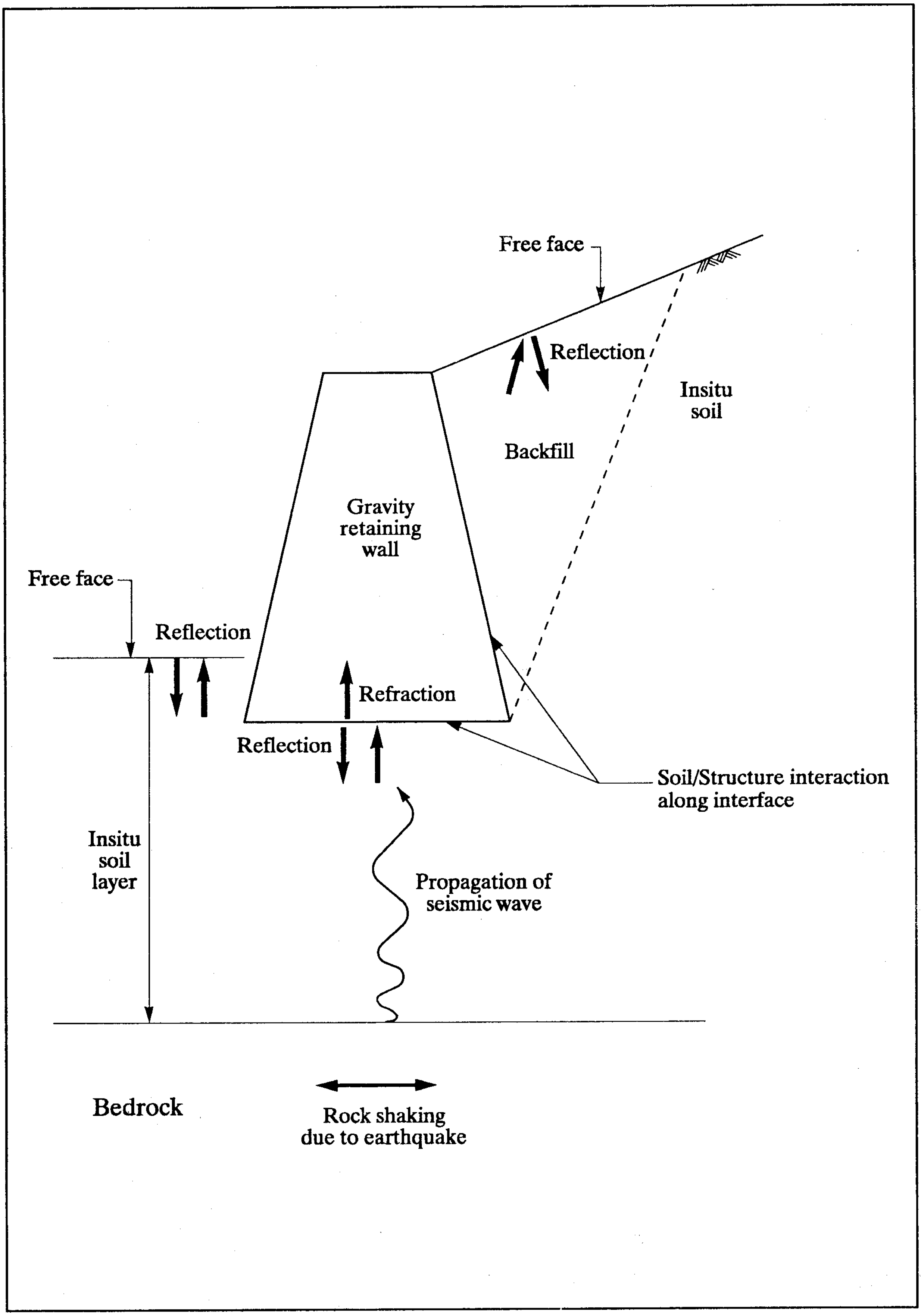

Figure 1 - Typical Gravity Retaining Wall Subject to Earthquake Loading

According to the Mononobe-Okabe solution,
the total dynamic force, P_{AE}, is given as follows :

$$P_{AE} = \frac{1}{2}\gamma H^2(1 + K_V)C_{AE}$$

Where

$$C_{AE} = \frac{\cos^2(\phi' - \theta - \beta)}{\cos\theta\ \cos^2\beta\ \cos(\delta + \beta + \theta)\left[1 + \sqrt{\frac{\sin(\phi' + \delta)\ \sin(\phi' - \theta - i)}{\cos(\delta + \beta + \theta)\ \cos(i - \beta)}}\right]^2}$$

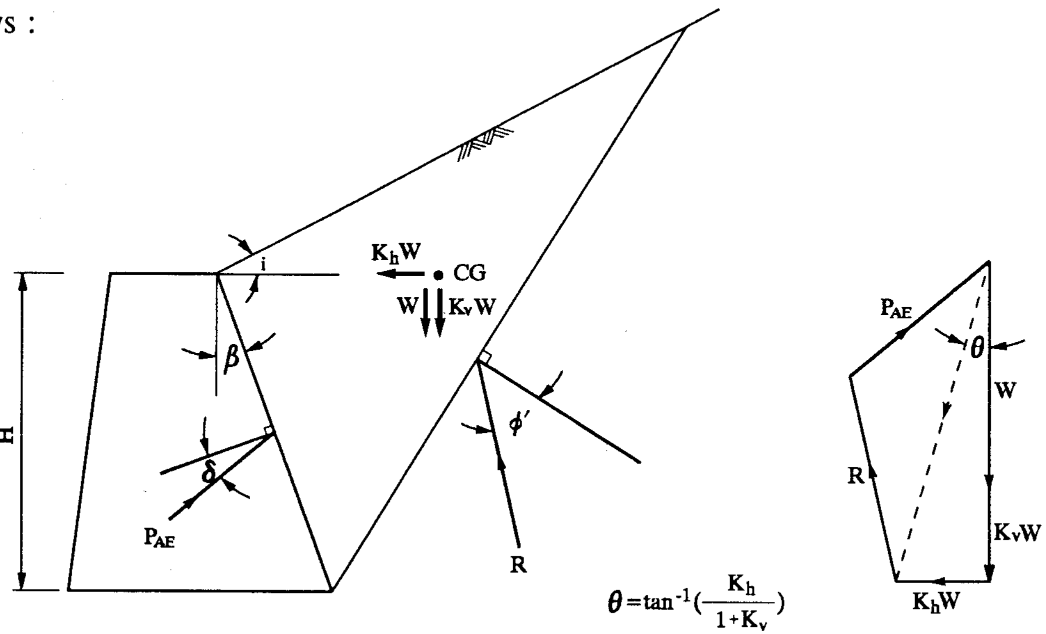

(a) Forces on Failure Wedge (b) Force Polygon

Legend :

CG	Centre of gravity	H	Hight of wall
K_h	Horizontal ground acceleration coefficient	ϕ'	Angle of shearing resistance of soil
K_v	Vertical ground acceleration coefficient	δ	Angle of wall friction
W	Weight of wedge	β	Inclination of back of wall to vertical
P_{AE}	Total dynamic force on retaining wall	γ	Unit weight of soil
R	Reaction on soil wedge from the surrounding ground	θ	Inclination of resultant inertial force to vertical
C_{AE}	Horizontal seismic coefficient	i	Inclination of ground surface behind wall to horizontal

Note : K_vW can also act vertically upwards.

Figure 2 - The Mononobe-Okabe Solution

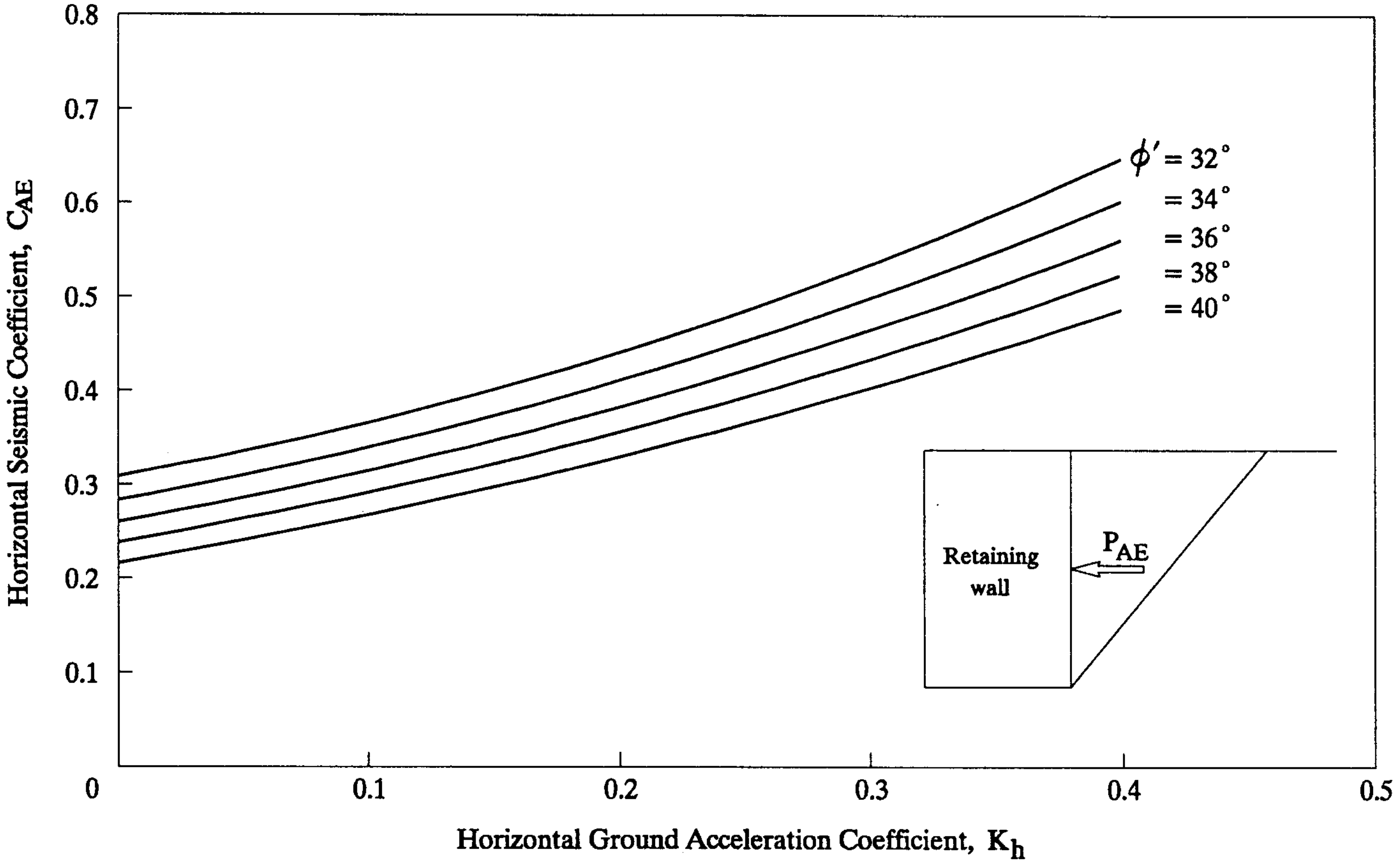

Figure 3 - Variation of C_{AE} with K_h for Different ϕ' (δ = zero)

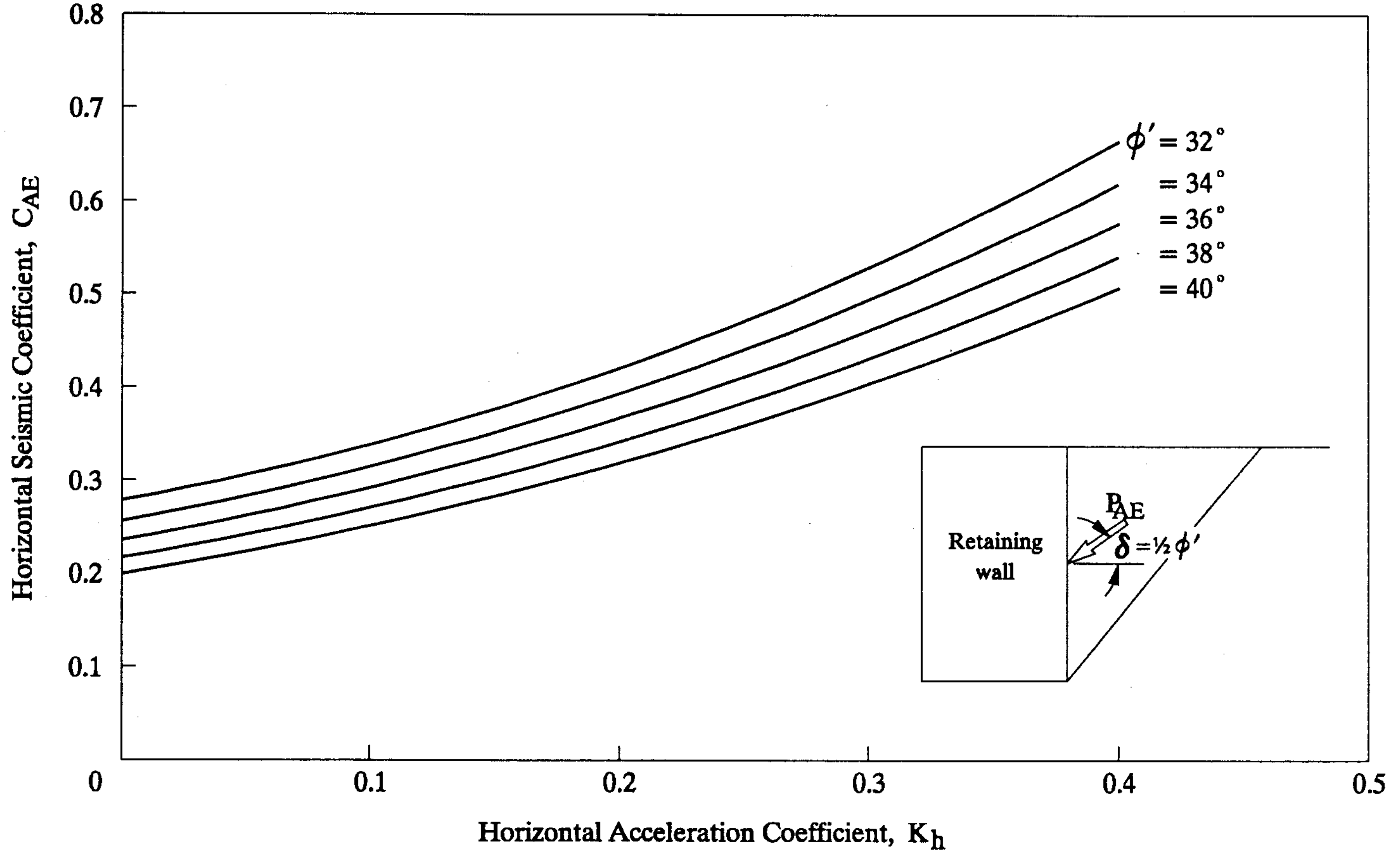

Figure 4 - Variation of C_{AE} with K_h for Different ϕ' ($\delta = 0.5\phi'$)

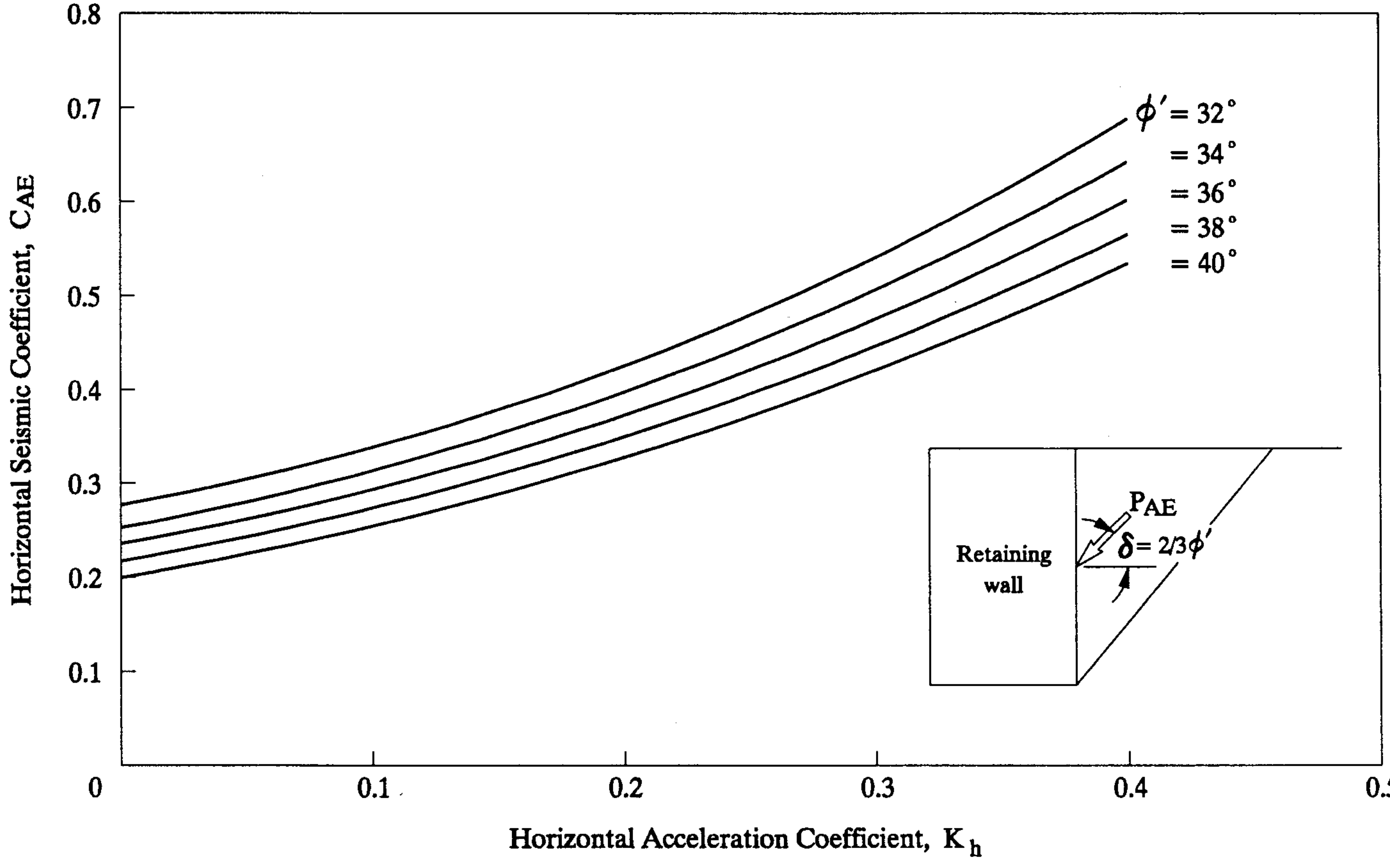

Figure 5 - Variation of C_{AE} with K_h for Different ϕ' ($\delta = 2/3\phi'$)

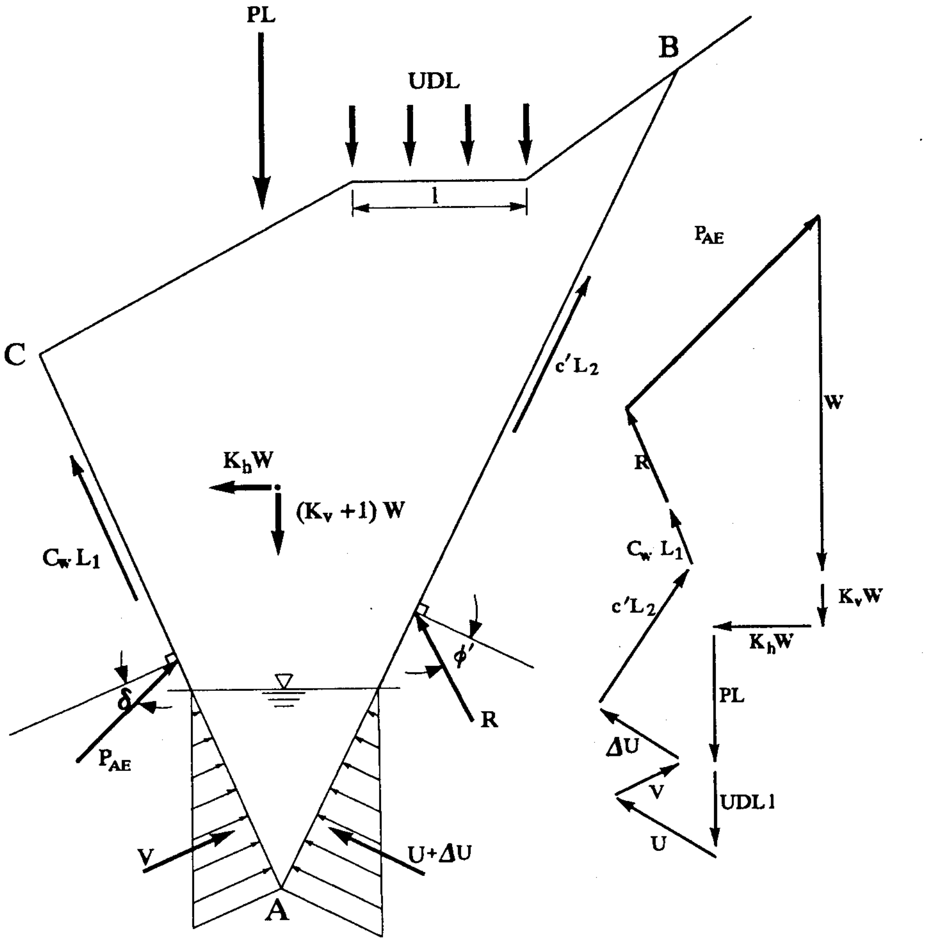

(a) Force Acting on Soil Wedge (b) Force Polygon

Legend :

PL	Point load
UDL	Uniformly distributed surcharge pressure
C_w	Wall adhesion
c'	Apparent cohesion of soil in terms of effective stress
V, U	Force due to water pressure
ΔU	Dynamic force due to excess water pressure
ϕ'	Angle of shearing resistance of soil
δ	Angle of wall friction
L_1	Length between points A & C
L_2	Length between points A & B

Notes : (1) V and U are static water forces on the wedge while ΔU is the dynamic force due to excess pore water pressure.
(2) Locked-in compaction stresses are not considered in the above illustration.
(3) See Figure 2 for the legend of symbols not defined above.

Figure 6 - Principle of Trial Wedge Analysis

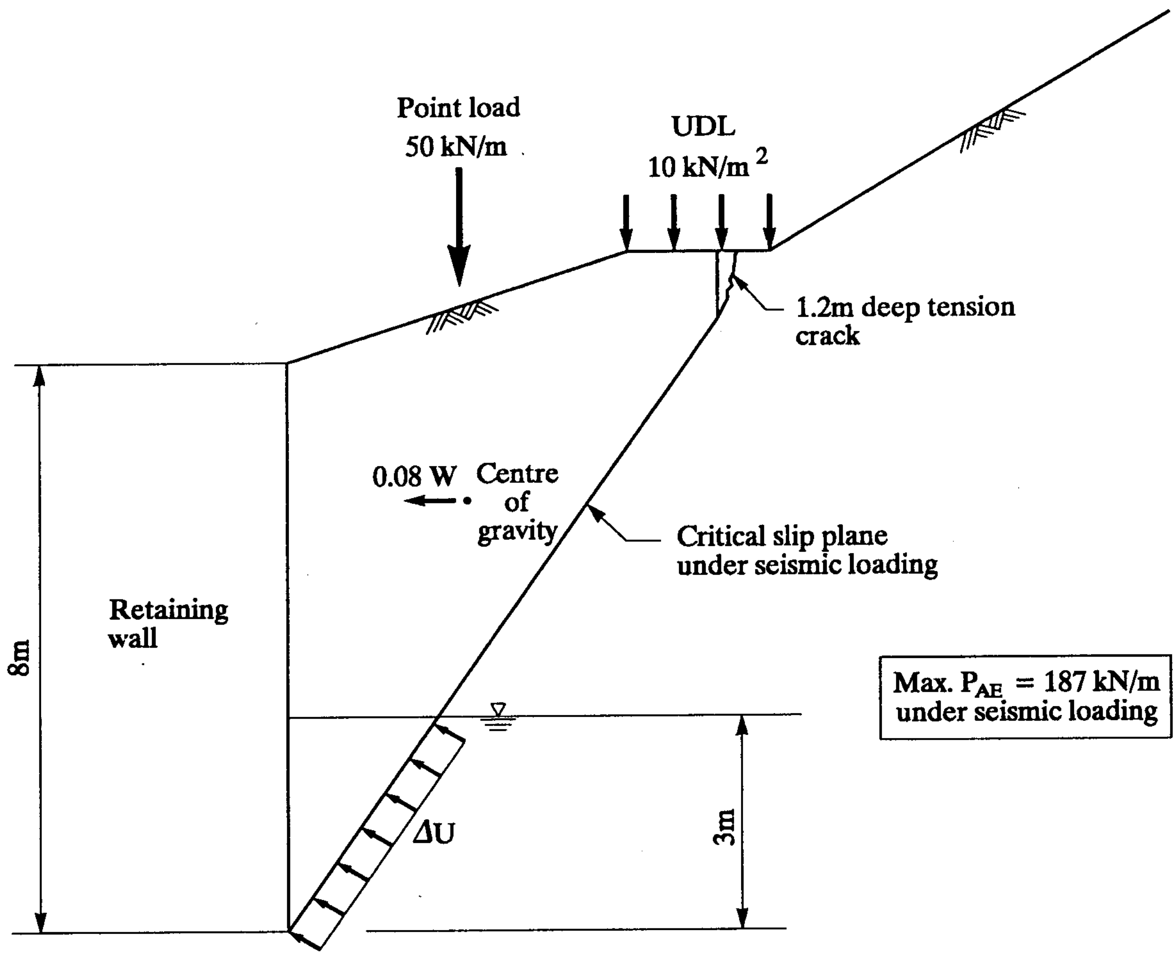

Notes : (1) An excess pore water pressure, ΔU, of 5 kN/m^2 has been allowed for in this example.
(2) See Figure 6 for legend of symbols.

Figure 7 - Example of Trial Wedge Analysis

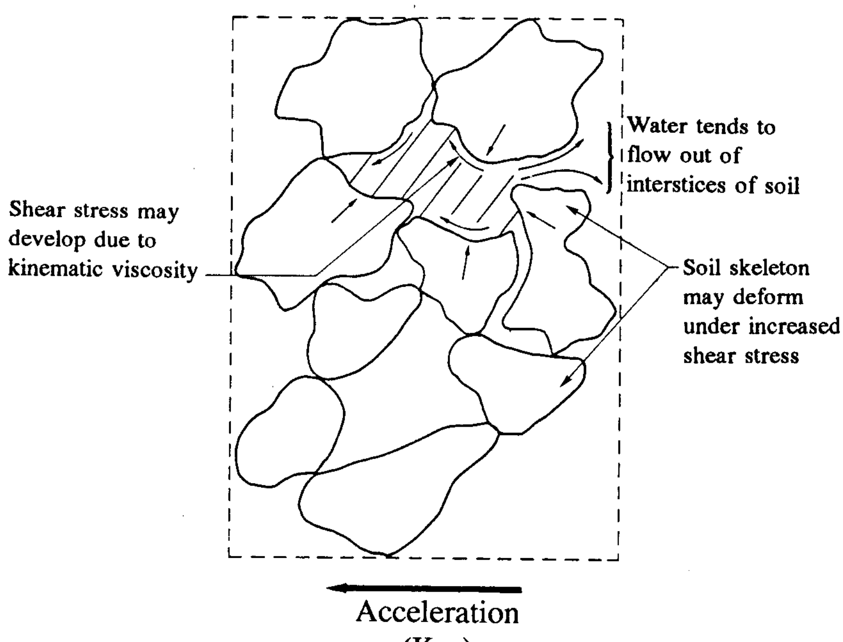

(a) Mechanisms of Change in Pore Water Pressure under Earthquake Loading

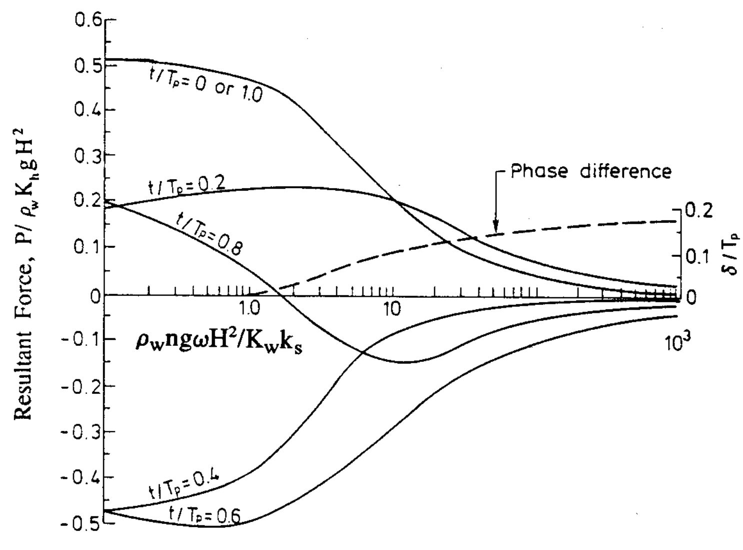

(b) Matsuo and O-Hara's (1965) Solution

Legend :

ω	$2\pi/T$	T_p	Period of vibration
n	Porosity of soil	H	Height of wall
ρ_w	Density of water	K_w	Bulk modulus of water
k_s	Permeability of soil	g	Acceleration due to gravity
K_h	Horizontal ground acceleration coefficient	P	Total force arising from dynamic pore water pressure
δ/T_p	Phase difference between forced vibration and dynamic pore water pressure	t	Time

Figure 8 - Matsuo and O-Hara's (1965) Solution for Dynamic Pore Water Pressure

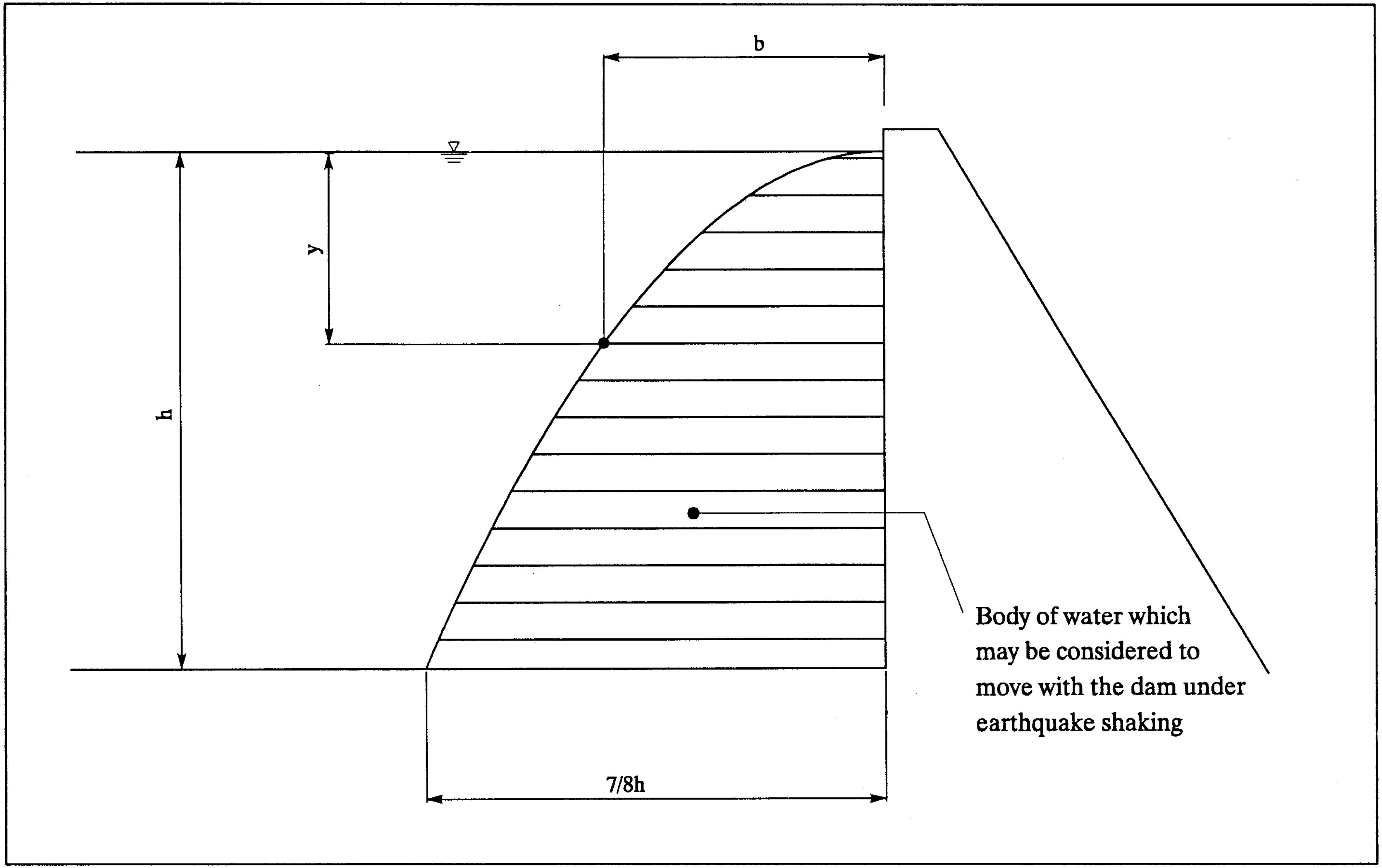

Figure 9 - Westergaard's (1933) Solution for Hydrodynamic Pressure

Values of Hydrodynamic Pressure Coefficient C_d				
y/h	cot m			
	0	2½	3	3½
0	0	0	0	0
0.1	0.24	0.04	0.035	0.027
0.2	0.35	0.08	0.07	0.06
0.3	0.45	0.12	0.10	0.08
0.4	0.53	0.15	0.14	0.11
0.5	0.6	0.18	0.16	0.14
0.6	0.65	0.21	0.18	0.16
0.7	0.688	0.22	0.20	0.17
0.8	0.7	0.22	0.20	0.17
0.9	0.72	0.2	0.18	0.15
1.0	0.73	0.14	0.11	0.10

$$p = C_d h K_h \gamma_w$$

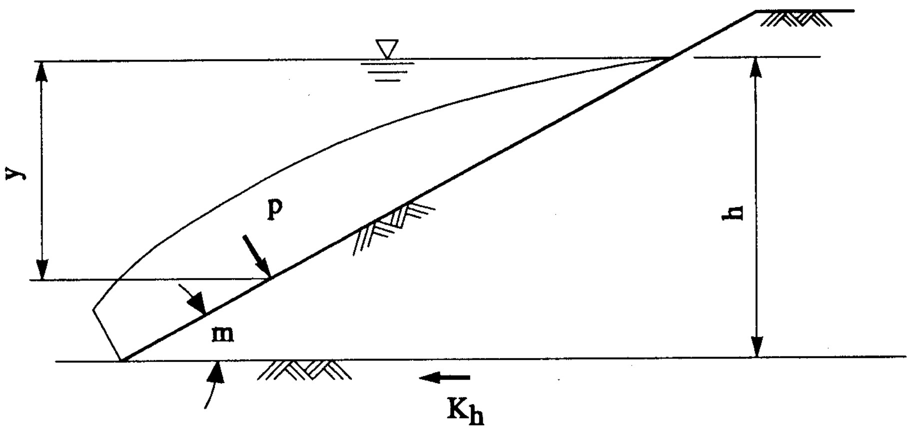

Legend :

- p Hydrodynamic pressure
- h Depth of water
- K_h Horizontal ground acceleration coefficient
- γ_w Unit weight of water
- C_d Hydrodynamic pressure coefficient

Figure 10 - Hydrodynamic Pressure on Inclined Water-retaining Structures

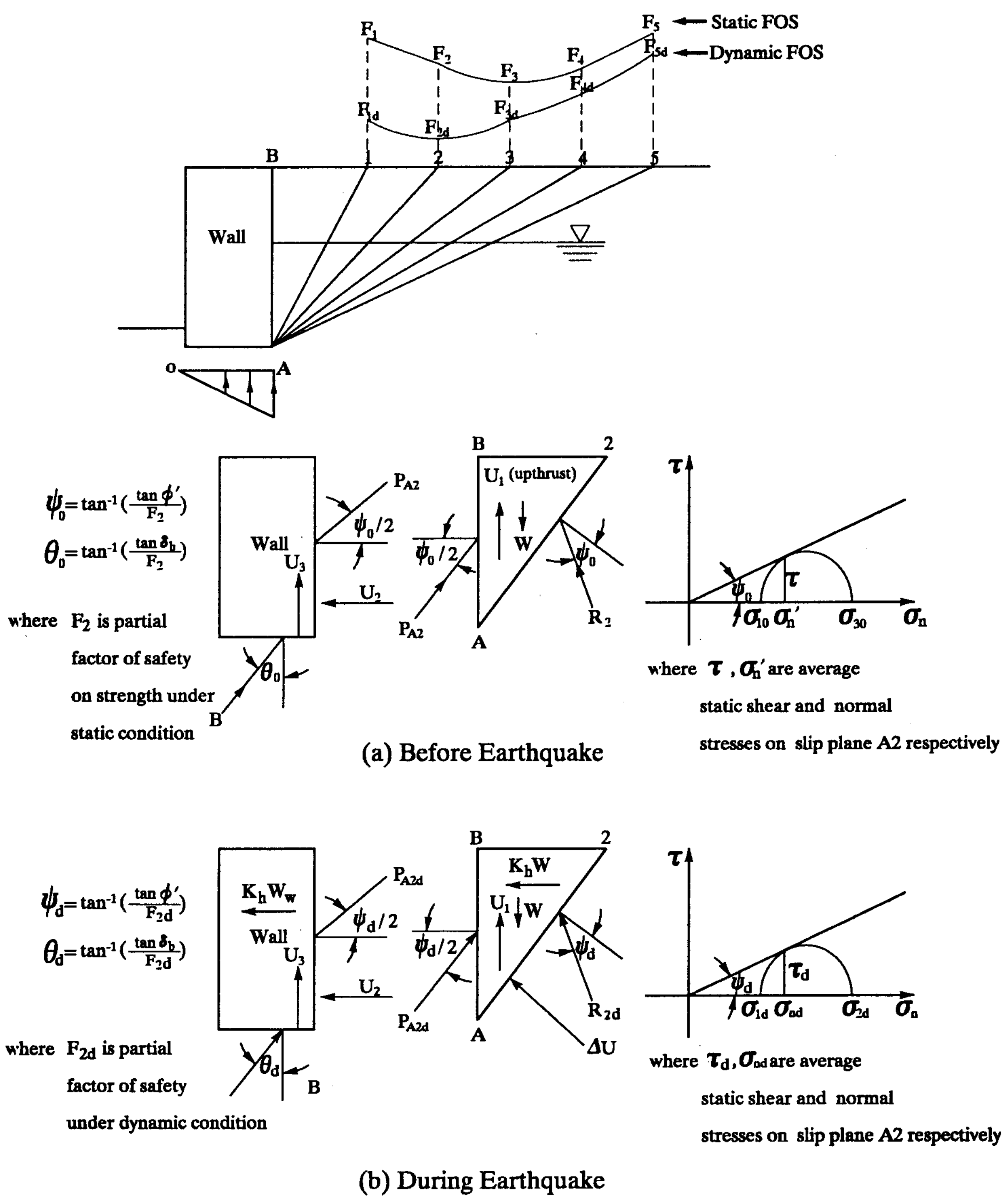

Notes :

(1) Assume mobilized friction angle is equal to ½ factored soil strength.
(2) U_1, U_2 & U_3 are static water forces.
(3) ΔU is dynamic water force due to excess pore water pressure generated under seismic loading.
(4) Forces are taken to be those at limiting equilibrium.

Figure 11 - Principle of Seismic Analysis of Retaining Wall Using Sarma's (1975) Approach

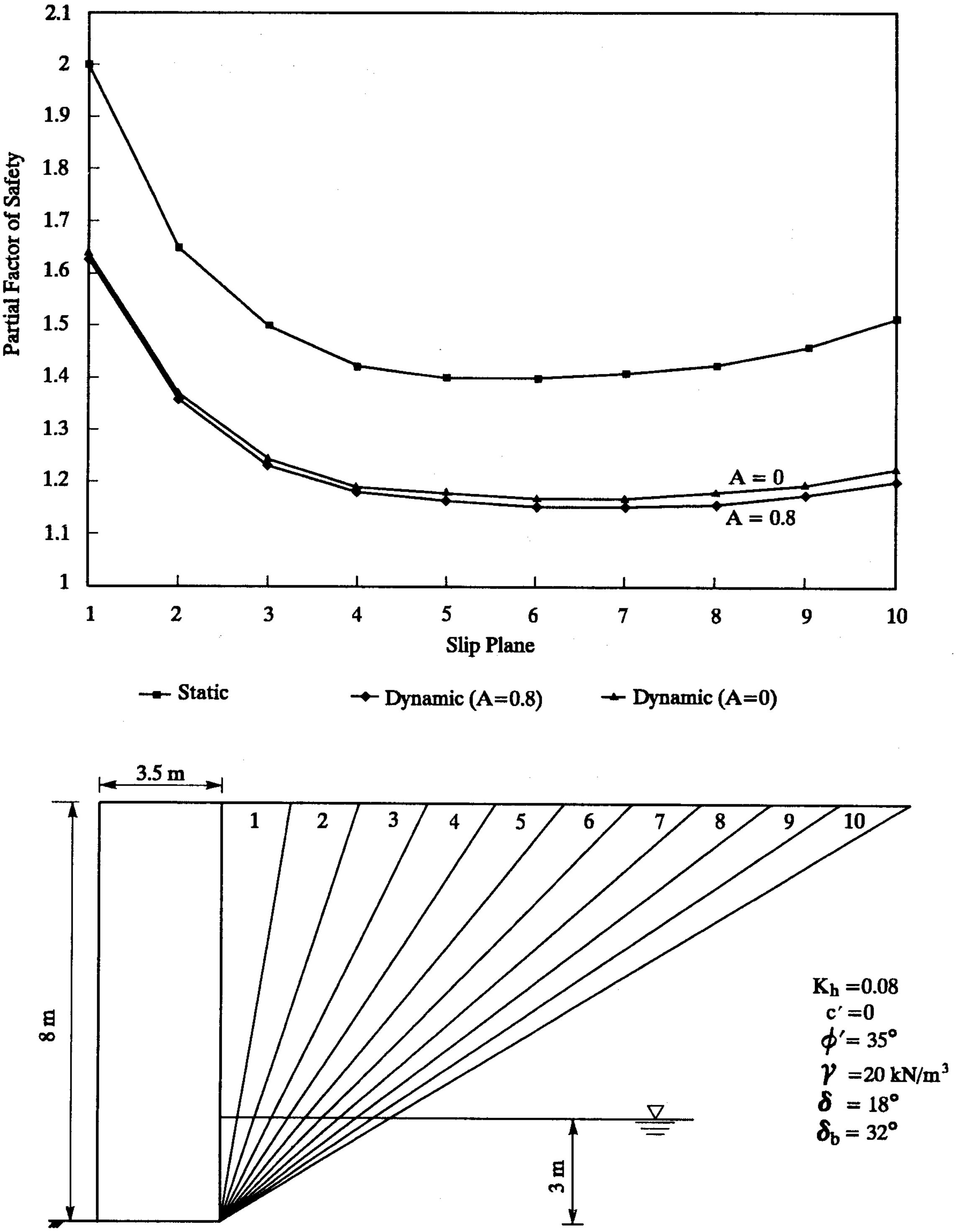

Legend :

δ	Angle of wall friction
δ_b	Angle of base shearing resistance
A	Skempton pore pressure parameter A

Note : See Figures 2 and 6 for the legend of symbols not defined above.

Figure 12 - Example of Seismic Analysis of Retaining Wall Using Sarma's Approach

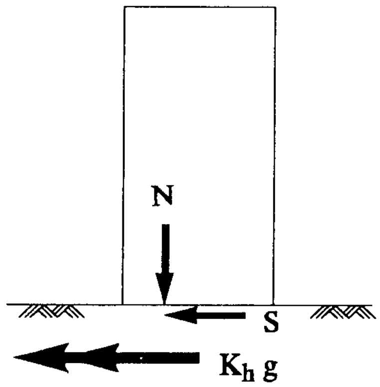

(a) Foundation Soil Subjected to Ground Acceleration K_h g

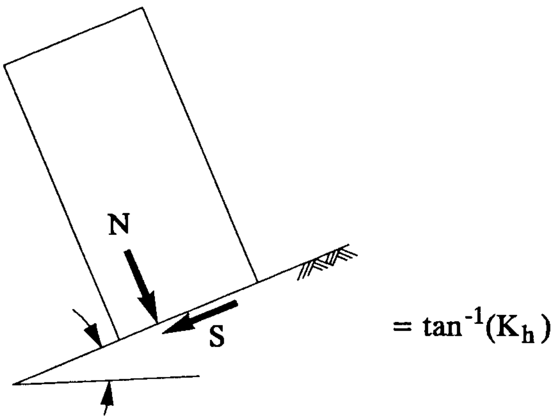

(b) Tilting of the Ground to Allow for Ground Acceleration

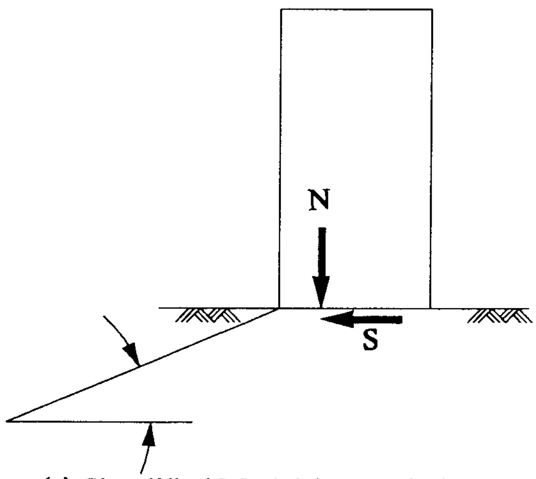

(c) Simplified Model for Analysis

Note : N, S are the resultant normal and shear forces respectively on the base of the wall which is subject to dynamic earth pressure.

Figure 13 - Simplified Model for Assessment of Bearing Capacity under Seismic Loading

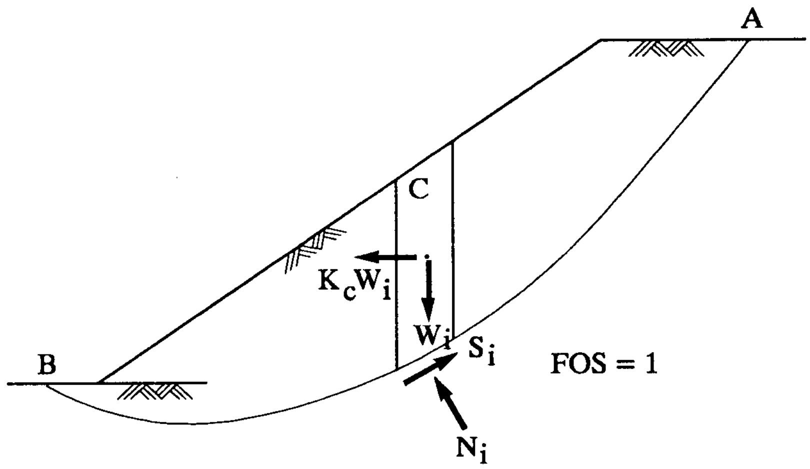

(a) Forces on Sliding Mass at Limiting Equilibrium under Seismic Loading

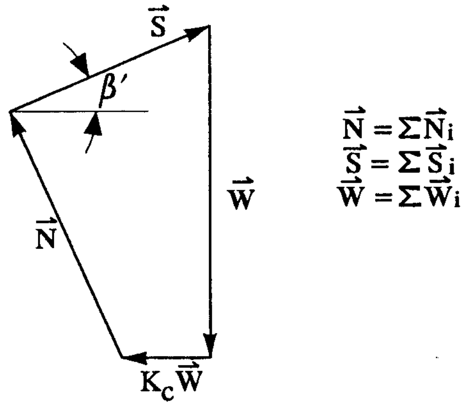

(b) Vector Force Diagram for FOS =1

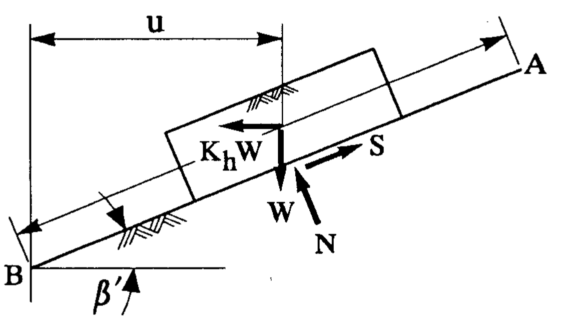

(c) Sliding of Equivalent Block Takes Place When FOS < 1 (i.e. $K_h > K_c$)

Note : Vertical acceleration assumed to be zero.

Figure 14 - Sliding Block Concept for Assessment of Displacement

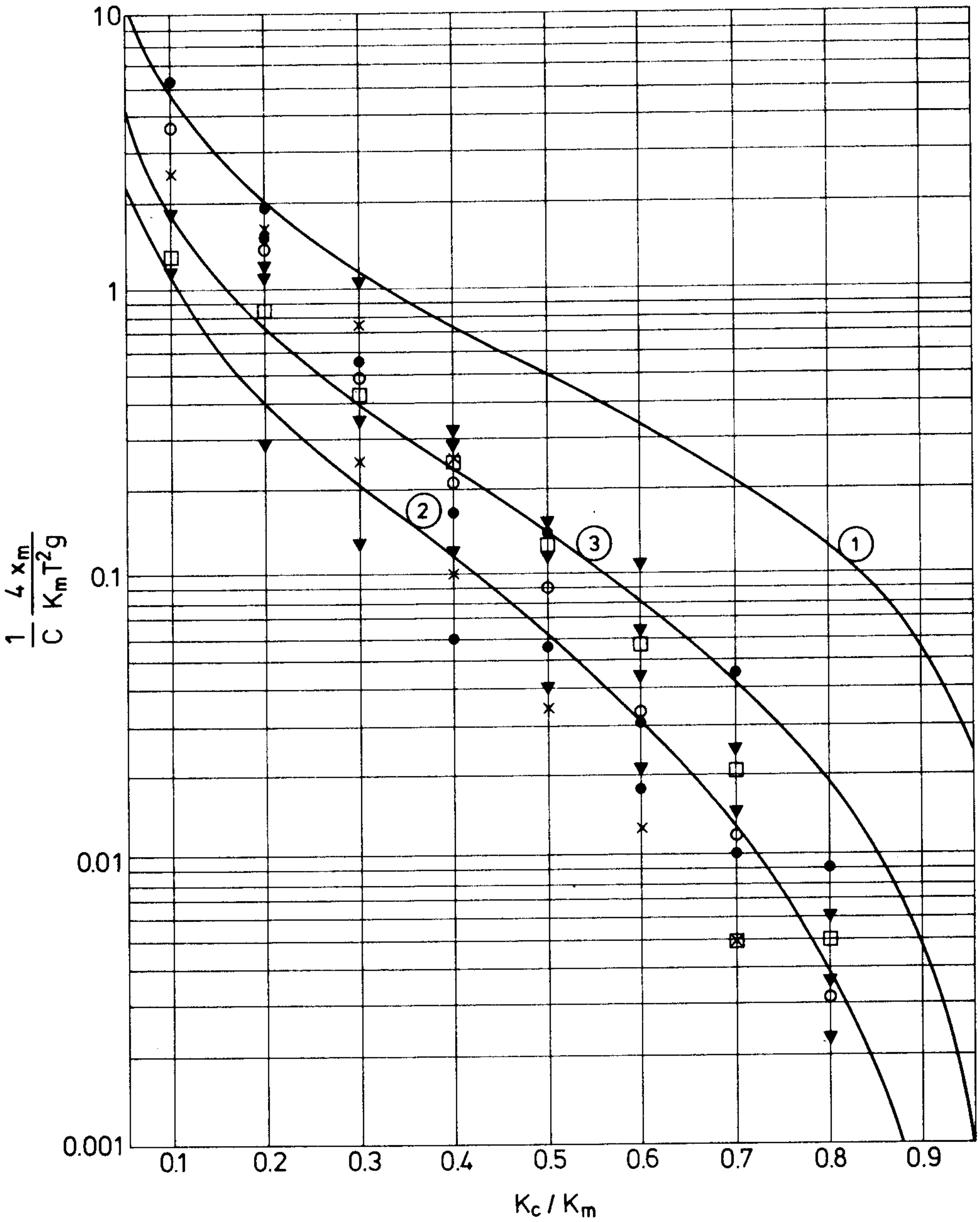

Legend :

1	Rectangular pulse	2	Triangular pulse
3	Half sine pulse	C	$\cos(\beta' \pm \theta' - \phi')/\cos\phi'$ (See Section 4.2)
o	El Centro 1940 (T = 0.5 sec)	•	Koyas 1967 (T = 0.15 sec)
×	Pacoima 1971 (T = 0.4 sec)	□	Parkfield 2 1966 (T = 0.6 sec)
▼	Several nuclear blasts	ϕ'	Angle of shearing resistance of soil
θ'	Inclination of resultant inertia force to horizontal	β'	Inclination of equivalent sliding plane to horizontal (see Figure 14)

Note : Figure after Sarma (1975).

Figure 15 - Plot of Dimensionless Displacement Function with K_c/K_m

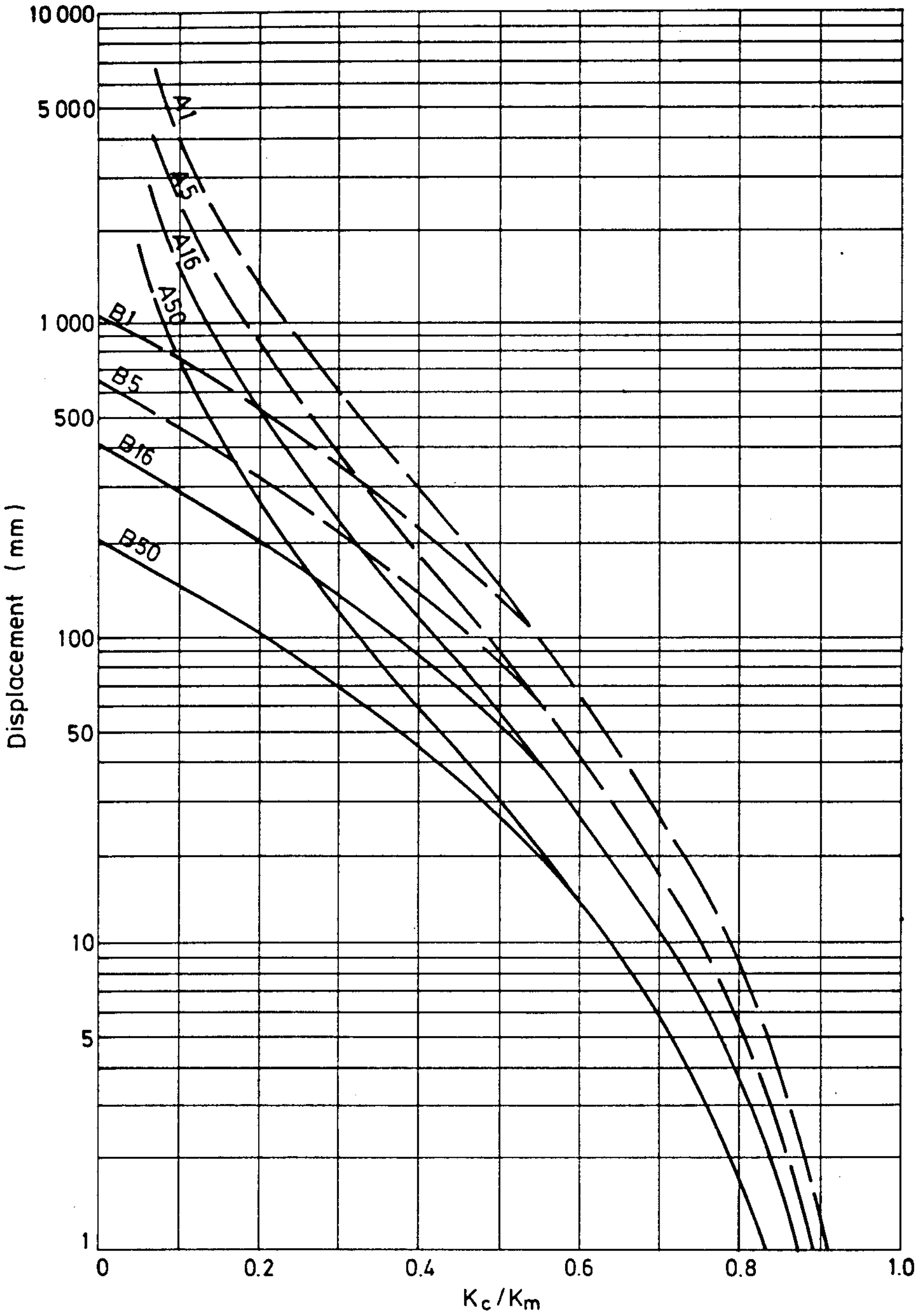

Legend :

K_c	Critical ground acceleration coefficient
K_m	Design ground acceleration coefficient
A_5	For slope } subscript denotes percentage probability of exceedance
B_5	For flat ground } subscript denotes percentage probability of exceedance

Notes : (1) Figure after Ambraseys & Menu (1988).
(2) For near-field earthquakes with magnitude ranging from 6.6 to 7.3.

Figure 16 - Plot of Sliding Displacement with K_c/K_m

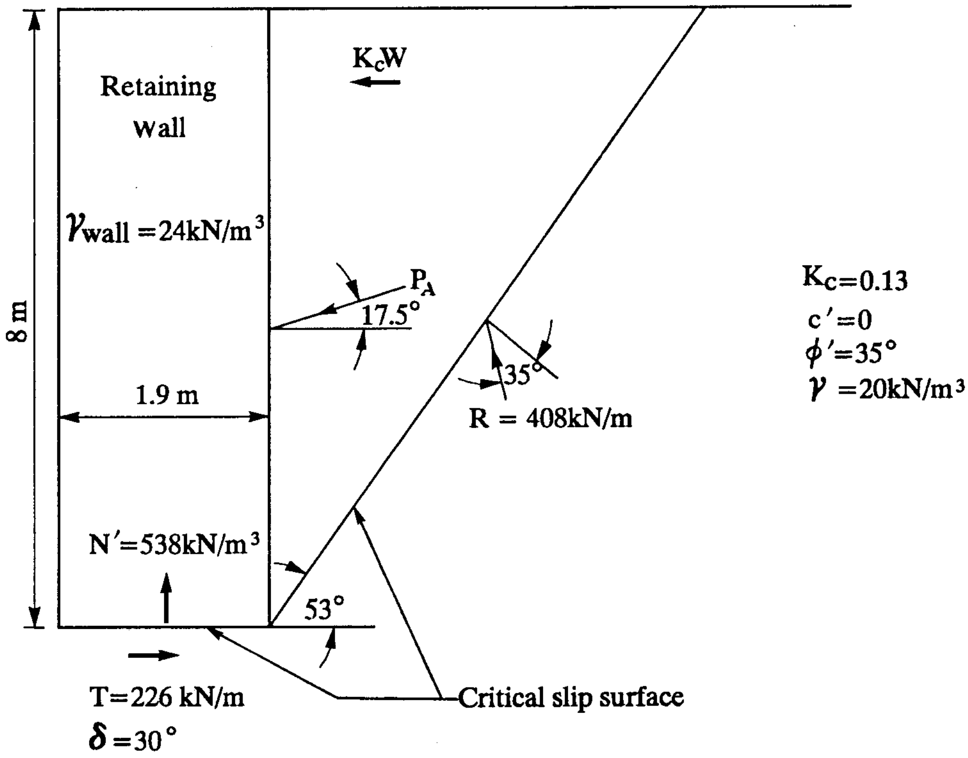

(a) Forces Acting on Wall

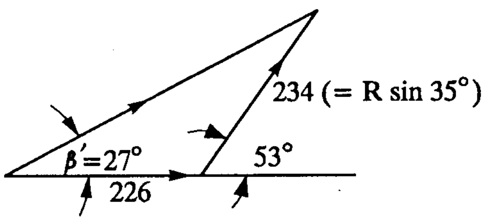

If $K_m = 0.2$ & $K_V = 0$

$$\frac{K_C}{K_m} = \frac{0.13}{0.2} = 0.65$$

From Fig 16, for 50% probability of exceedance, $X_m = 8$ mm

(b) Ambraseys and Menu (1988) Method

$$C = \frac{\cos(27° - 35°)}{\cos 35°} = 1.21 \quad \rightarrow \quad \frac{4\,x_m}{CK_m T^2 g} = f$$

From Figure 15 (Sarma's solution)	For T=0.2 s
Rectangular pulse	6.4 mm
Half-sine pulse	1.4 mm
Triangular pulse	0.5 mm
From Equation 12, $x_m = 0.0157\,T^2$	0.9 mm

[f can be read off from Figure 15 or calculated from Equation 12]

(c) Sarma's (1975) Method

Figure 17 - Assessment of Sliding Displacement of Retaining Wall under Seismic Loading

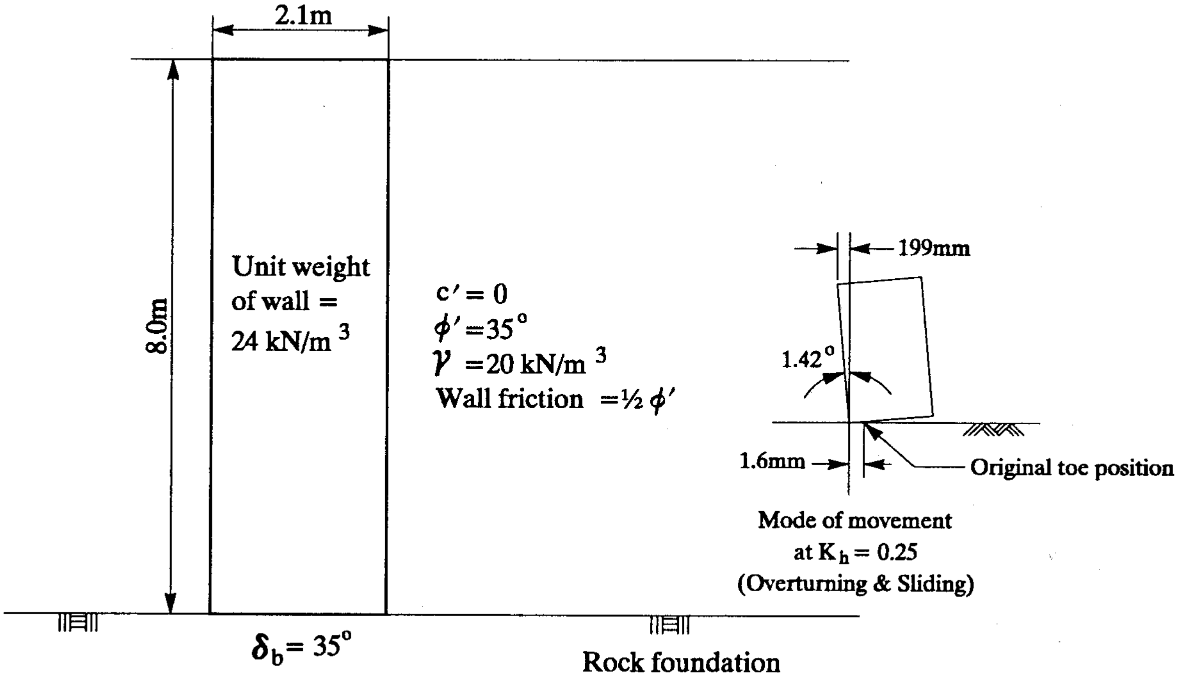

K_h	FOS	Horizontal Displacement (mm)	Rotation about Toe (deg)
0.03	> 1	0	0
0.25	< 1	1.6	1.42° (199mm displacement at top of wall)

Notes : (1) Where the factor of safety is less than unity, Equation 12 is used assuming T = 0.2 sec for deformation assessment.
(2) Bearing stability is deemed to be satisfactory as wall is founded on rock.
(3) K_c is calculated to be 0.04 for overturning and 0.22 for sliding.

Figure 18 - Example of Analysis of Sliding Displacement and Rotation of Gravity Retaining Wall - Case 1

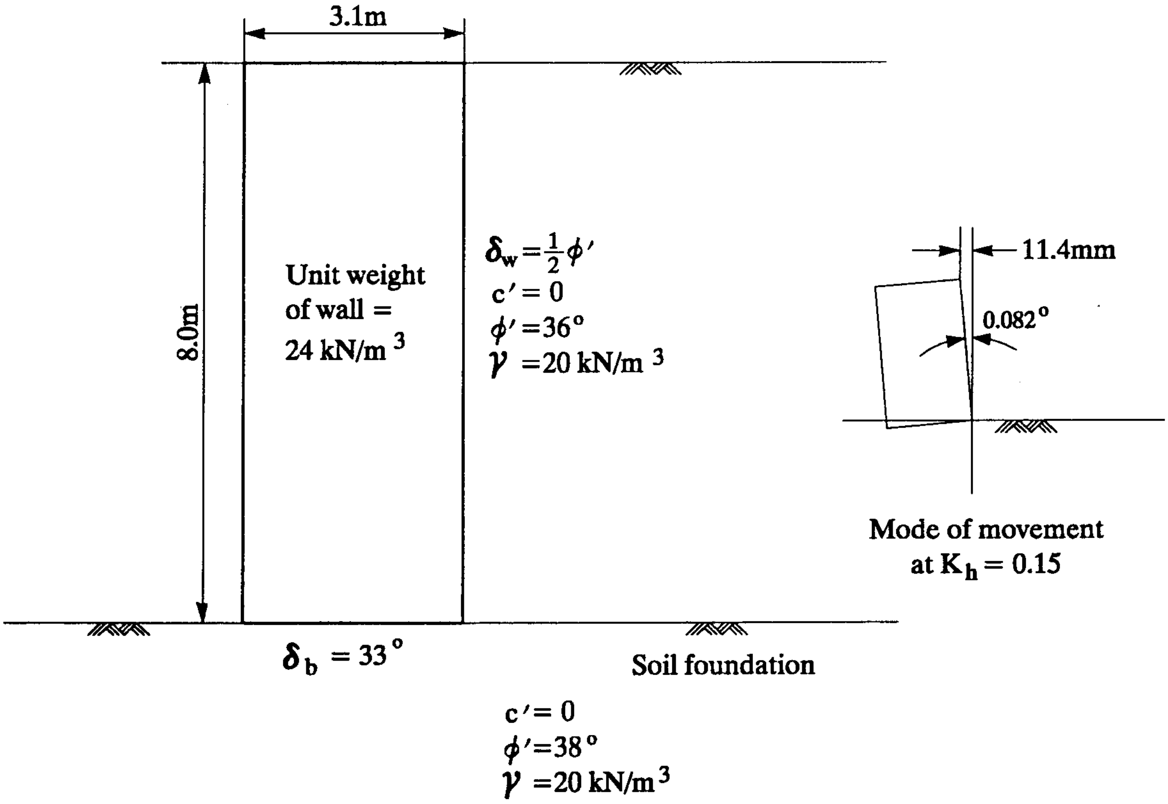

K_h	FOS	Horizontal Displacement (mm)	Rotation about Heel (Deg)
0.05	> 1	0	0
0.15	< 1	0	0.082° (11.4mm displacement at top of wall)

Notes : (1) Where the factor of safety is less than unity, Equation 12 is used assuming T = 0.2 sec for deformation assessment.
(2) K_c is calculated to be 0.062 for bearing capacity.

Figure 19 - Example of Analysis of Sliding Displacement and Rotation of Gravity Retaining Wall - Case 2

APPENDIX A

SEISMIC STABILITY ANALYSIS OF RETAINING WALL USING SARMA'S (1975) APPROACH

Seismic Stability Analysis of Retaining Wall Using Sarma's (1975) Approach

Under static conditions, it is assumed that the Mohr circle of stresses along plane A2 just touches the line which inclines at an angle of ψ_0 to the axis of normal stress (Figure 11).

Therefore, the principal stresses before seismic excitation, σ_{10} and σ_{30}, are given as follows :

$$\sigma_{10} = \sigma_n + \tau\,(\tan\psi_0 + \sec\psi_0) \quad \text{(A1)}$$
$$\sigma_{30} = \sigma_n + \tau\,(\tan\psi_0 - \sec\psi_0) \quad \text{(A2)}$$

where σ_n, τ is the average normal and shear stress along plane A2 respectively.

Under the seismic load, K_h W,

$$\sigma_{1d} = \sigma_{nd} + \tau_d\,(\tan\psi_0 + \sec\psi_0) \quad \text{(A3)}$$
$$\sigma_{3d} = \sigma_{nd} + \tau_d\,(\tan\psi_0 - \sec\psi_0) \quad \text{(A4)}$$

where σ_{1d} and σ_{3d} are the principal stresses under dynamic conditions.

Now,

$$\Delta\sigma_1 = \sigma_{1d} - \sigma_{10}$$
$$\Delta\sigma_3 = \sigma_{3d} - \sigma_{30}$$

and using Skempton's equation, the excess (or dynamic) pore water pressure, Δu, is given by the following :

$$\Delta u = \Delta_3 + A(\Delta\sigma_1 - \Delta\sigma_3) \quad \text{if } B=1$$
$$= \sigma_{3d} - \sigma_{30} + A(\Delta\sigma_{1d} - \sigma_{10} - \sigma_{3d} + \sigma_{30}) \quad \text{(A5)}$$

Substituting (A1), (A2), (A3) & (A4) into (A5),

$$\Delta u = \sigma_{nd} + \tau_0(\tan\psi_d - \sec\psi_d + 2A\sec\psi_d) - X \quad \text{(A6)}$$

where $X = \sigma_n + \tau(\tan\psi_0 - \sec\psi_0) + 2A\tau\sec\psi_0$

It is assumed that R_{2d} is the effective resultant force on plane A2 under dynamic condition, and that the Mohr circle of stresses just touches the line inclined at an angle of ψ_d to the axis of normal stress. It is further assumed that τ_d and σ_{nd} are uniformly distributed, i.e.

$$\tau_d = (R_{2d}\sin\psi_d)/L \quad \text{(A7)}$$
$$\sigma_{nd} = (R_{2d}\cos\psi_d)/L \quad \text{(A8)}$$

Substitute (A7) & (A8) into (A6),

$$\Delta u = R_{2d}\,[\cos\psi_d/L + \sin\psi_d/L\,(\tan\psi_d - \sec\psi_d + 2A\sec\psi_d)] - X \quad \text{(A9)}$$

$\Delta u \quad = (R_{2d}\,Y) - X$

where $Y = \cos\psi_d/L + \sin\psi/L\ (\tan\psi_d - \sec\Psi_d + 2A\ \sec\psi_d)$

The total dynamic water force ΔU is given by the following :

$\Delta U \quad = \Delta u^*L'$ (L'is the saturated length of plane A2 that is below the water table)

$= (R_{2d}\,Y - X)\,L'$ . . . . (A10)

Now consider the force equilibrium of wedge AB2 under seismic loading (Figure A1)

Total Weight $W = \frac{1}{2}\,H^2\,\frac{1}{\tan\eta}\,\gamma$

Static Water Force $U_1 = \frac{1}{2}\,H_w^2\,\frac{1}{\tan\eta}\,\gamma_w$

<u>For Vertical force equilibrium</u>

$W \quad = P_{A2d}\sin(\psi_d/2) + R_{2d}\sin(90\text{-}\eta+\psi_d) + \Delta U\cos\eta + U_1$ . . . . (A11)

<u>Horizontal force equilibrium</u>

$K_hW + R_{2d}\cos(90\text{-}\eta+\psi_d) + \Delta U\sin\eta = P_{A2d}\cos\psi_d/2$ . . . . (A12)

Substituting (A10) into (A11) and (A12) and rearranging the terms,

$P_{A2d}\sin(\psi_d/2) + R_{2d}[\sin(90\text{-}\eta+\psi_d)+YL'\cos\eta] = W + XL'\cos\eta - U_1$ . . . . (A13)

$P_{A2d}\cos(\psi_d/2) - R_{2d}[\cos(90\text{-}\eta+\psi_d)+YL'\sin\eta] = K_hW - XL'\sin\eta - U_1$ . . . . (A14)

According to Equations (A13) and (A14), P_{A2d} is a function of partial safety factor F_{2d} under the seismic loading K_h W. At the same time, P_{A2d} is also a function of the partial safety factor on base friction with respect to wall sliding.

Therefore, a trial and error procedure needs to be adopted, and the correct F_{2d} is that which gives the same P_{A2d} for limiting equilibrium of the soil wedge and the retaining wall.

LIST OF FIGURES

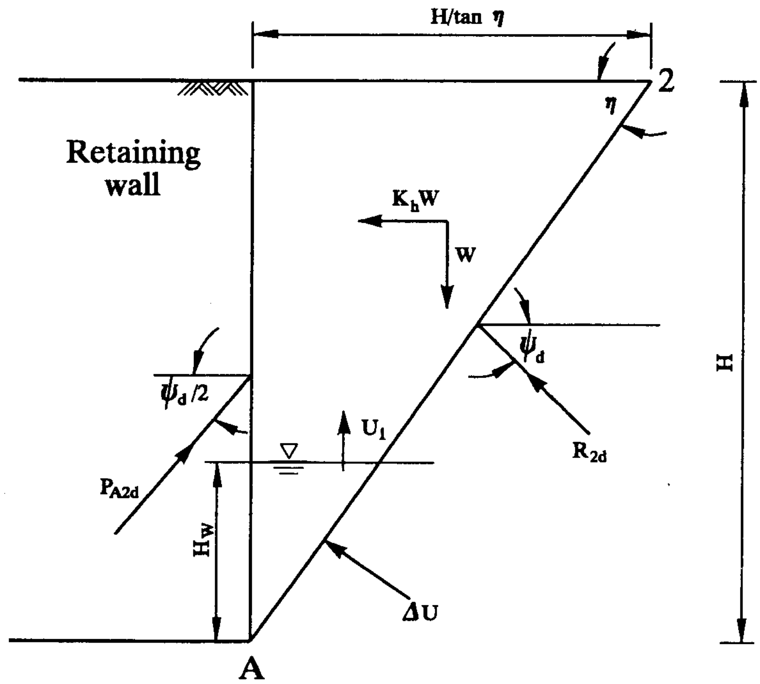

Legend :

H	Height of wall
H_w	Height of water table above wall base
U_1	Static water force
ΔU	Excess water force due to earthquake
η	Angle of sliding surface with horizontal

Note : See Figure 11 for definition of symbols not given above.

Figure A1 - Forces Acting under Seismic Loading

APPENDIX B

DERIVATION OF PROPOSED METHODOLOGY FOR ASSESSING DYNAMIC WALL ROTATION

Derivation of Proposed Methodology for Assessing Dynamic Wall Rotation

In this Appendix, the equations for estimating of the wall rotation are derived for situations when the overturning moment exceeds the restoring moment under seismic loading (Figure B1)

Overturning moment, M_1, due to static earth pressure

$M_1 = P_s \cos\delta \, h_1 - P_s \sin\delta \, B$ . . . . (B1)

Overturning moment, M_2, due to dynamic pressure increment

$M_2 = P_{dyn} \cos\delta \, h_2 - P_{dyn} \sin\delta \, B$ . . . . (B2)

Overturning moment, M_3, due to seismic loading K_h W

$M_3 = K_h \, W \, H/2$ . . . . (B3)

Restoring moment, M_r,

$M_r = W \, B/2$ . . . . (B4)

Now, net overturning moment $M_0 = M_1 + M_2 + M_3 - M_r$

$M_0 = P_s [\cos\delta \, h_1 - \sin\delta \, B] + P_{dyn} [\cos\delta \, h_2 - \sin\delta \, B] +$
$K_h \, W \, H/2 - W \, B/2$ . . . . (B5)

By definition, K_c corresponds to the case when $M_0 = 0$.

From Equation (B5),

$P_s [\cos\delta \, h_1 - \sin\delta \, B] + P_{kc}[\cos\delta \, h_2 - \sin\delta \, B] +$
$K_c \, W \, H/2 - W \, B/2 = 0$ . . . . (B6)

where P_{kc} is dynamic force when $K_h = K_c$.

Equation (B5) minus Equation (B6) :

$M_0 = (P_{dyn} - P_{kc}) (h_2 \cos\delta - B \sin\delta) + (K_m - K_c) \, W \, H/2$ . . . . (B7)

Given that $P_{dyn} = 1/2 \, \gamma \, H^2 \, (C_{AE} - C_0)$

$P_{kc} = 1/2 \, \gamma H^2 \, (C_{kc} - C_0)$

where C_0, C_{kc}, C_{AE} are the horizontal seismic coefficients with $K_h=0$, $K_h = K_c$ and $K_h = K_m$ respectively.

As shown in Figures 3 to 5, C_{AE} can reasonably be assumed to have a linear relationship with K_h, for K_h up to about 0.2. Thus,

$$C_{AE} = C_0 + \mu K_m$$

$$C_{kc} = C_0 + \mu K_c$$

and therefore

$$P_{dyn} = 1/2 \gamma H^2 \mu K_m$$

$$P_{kc} = 1/2 \gamma H^2 \mu K_c$$

Substituting into Equation (B7)

$$M_0 = 1/2 \gamma H^2 \mu (h_2 \cos\delta - B \sin\delta) (K_m - K_c) + (K_m - K_c) W H/2$$

$$M_0 = [1/2 \gamma H^2 \mu (h_2 \cos\delta - B \sin\delta) + W H/2] (K_m - K_c) \qquad \text{(B8)}$$

Therefore, the angular acceleration $\ddot{\Theta}$ of the wall is

$$\ddot{\Theta} = M_0 / I$$

$$\ddot{\Theta} = [1/2 \gamma H^2 \mu (h_2 \cos\delta - B \sin\delta) + W H/2]/I (K_m - K_c) \qquad \text{(B9)}$$

$$= D (K_m - K_c)$$

Now, Sarma's basic equation for assessment of displacements is :

$$a = g \cos(\beta' - \theta' - \phi)/\cos\phi (K_m - K_c)$$

$$= g C (K_m - K_c) \qquad \text{(B10)}$$

The two Equations (B9) and (B10) have the same form with the displacement acceleration replaced by angular acceleration and the term "C g" replaced by D.

As Sarma has produced solutions for the dimensionless displacement term, $4x_m/CK_mT^2g$, the same solution can be used to give angular displacement or rotation with the term "C g" replaced by D.

LIST OF FIGURES

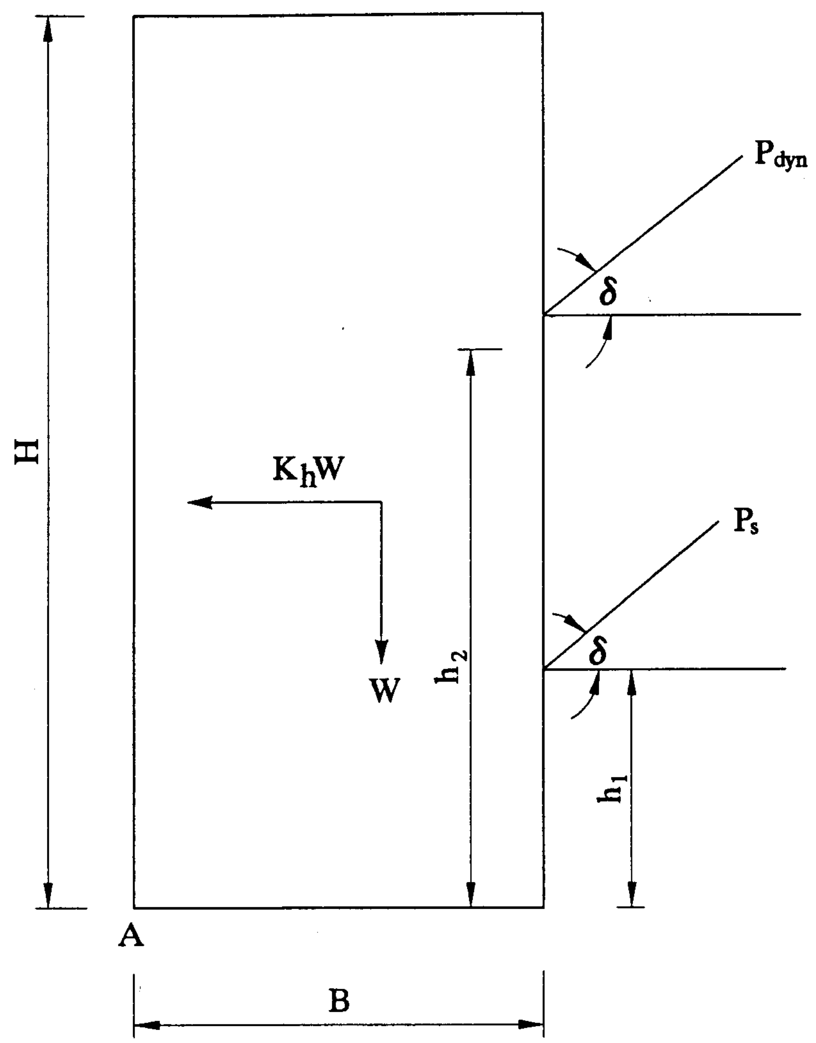

Legend :

P_{dyn}	Dynamic force when $K_h = K_m$
K_m	Maximum ground acceleration coefficient
P_s	Static earth pressure
P_{kc}	Dynamic force when $K_h = K_c$

Notes : (1) Vertical ground acceleration assumed to be zero.
(2) Static and dynamic angles of wall friction are taken to be the same.

Figure B1 - Pressure Acting on the Back of Retaining Wall under Seismic Loading